Advancements in Piezoelectric-Enabled Devices for Optical Communication

Agata Roszkiewicz,* Magdalena Garlińska, and Agnieszka Pregowska

The ability of piezoelectric materials to convert mechanical energy into electric energy and vice versa has made them desirable in the wide range of applications that oscillate from medicine to the energetics industry. Their implementation in optical communication is often connected with the modulation or other manipulations of the light signals. In this article, the recent advancements in the field of piezoelectrics-based devices and their promising benefits in optical communication are explored. The application of piezoelectrics-based devices in optical communication allows dynamic control, modulation, and manipulation of optical signals that lead to a more reliable transmission. It turns out that a combination of artificial-intelligence-based algorithms with piezoelectrics can enhance the performance of these devices, including optimization of piezoelectric modulation, adaptive signal processing, control of optical components, and increase the level of energy efficiency. It can enhance signal quality, mitigate interference, and reduce noise-connected issues. Moreover, this technological fusion can increase the security of optical communication systems. Finally, the potential future research lines are determined.

1. Introduction

Piezoelectricity was discovered in 1880 by French physicists Jacques and Pierre Curie.[1] The piezoelectric effect is based on the appearance of the electric charge at the surface of some materials in response to the applied mechanical stress or pressure. The inverse piezoelectric effect is the mechanical deformation of a material as a result of applied voltage. Progress in their development has made it possible to control the optical processes occurring in them, both as features of a given material and as a triggering disturbance.[2] The unquestionable advantage of using piezoelectrics is the ability to minimize the size of the devices.[3] Thus, piezoelectric materials find their application in many fields of science and technology, including microelectronics, mechanical engineering, optics, photonics, life sciences, biology, and

A. Roszkiewicz, A. Pregowska
Institute of Fundamental Technological Research
Polish Academy of Sciences
Pawinskiego 5B Str., 02-106 Warsaw, Poland
E-mail: arosz@ippt.pan.pl

M. Garlińska
Łukasiewicz Centre
Poleczki Str. 19, 02-822 Warsaw, Poland

The ORCID identification number(s) for the author(s) of this article can be found under https://doi.org/10.1002/pssa.202400298.

medicine, in particular, endodontic microsurgery[4] or neuroprosthetic devices.[5] The development of the fifth-generation mobile networks (5G) contributes to the group of spectacular applications that are connected with optical communication, which encompass large-range optical intersatellite communication, deep space optical communication, free space optical communication (FSO) as well as optical communication at small distances that are characterized with low-power consumption and the low productions cost.[6]

Optical communication utilizes a modulated monochromatic light beam to send information from a transmitter to a receiver. It encompasses a broad range of the electromagnetic (EM) spectrum, from 10 THz to 1 EHz, which corresponds to the range from far infrared to near-ultraviolet.[7] The general term "optical communication" is not limited only to a relatively narrow wavelength range of optical windows (850, 1310, and 1550 nm) covered by optical fiber communication. We consider all EM wavelengths that are used to transmit signals, from infrared to ultraviolet light.

It is estimated that we know about several tens of thousands of materials with piezoelectric properties. Piezoelectric properties can be found both in a single crystal and polycrystals (ceramics) composed of the same material (e.g., quartz, GaAs, GaN, BN, InN, AlN, CdS, CdSe, ZnO, MoS_2, lead zirconate titanate (PZT), $BiFeO_3$, ZrO_2, TiO_2, $NaNbO_3$, $KNaNbO_3$, $LiNbO_3$, Na_2WO_3, $LiTaO_3$, $BaTiO_3$, $NaBi(TiO_3)_2$, $Bi_4Ti_3O_{12}$, $Pb_2KNb_5O_{15}$, $Ba_2NaNb_5O_5$).[8,9] Also, some organic substances like polymers (poly (L-lactic acid), polyvinylidene fluoride [PVDF], poly(vinylidene difluoride–trifluoroethylene) [P(VDF–TrFE]), polydimethylsiloxane, poly-β-hydroxybutyrate, poly(3-hydroxybutyrate-co-3-hydroxyvalerate)) and biomolecules (silk, β-glycine, chitin, collagen, cellulose, peptides, proteins, viruses, amino acids, diphenylalanine, DNA, bones) show piezoelectric properties. There are also nonconventional piezoelectric materials, like organic–inorganic hybrid materials, composite materials (PZT–polymer composites, ceramic–metal composites, etc.), nanomaterials (nanowires, nanotubes, etc.), or 2D materials (graphene, etc.). **Figure 1** presents some of the materials that show piezoelectricity.

Piezoelectric ceramics are a class of materials composed of multiple crystals or grains that are oriented randomly. They are made by sintering the powders of piezoelectric materials which results in fused solid bulk material. This random

orientation gives ceramics some unique properties, such as high hardness, strength, and higher tolerance of impurities and defects compared to single crystals, but it also reduces their piezoelectric properties. Randomly oriented polycrystalline ceramics can only exhibit piezoelectricity if they are ferroelectric. Consider polycrystalline ZnO thin films, which possess a wurtzite structure and exhibit piezoelectric and pyroelectric properties but no ferroelectric. This remarkable behavior arises from the alignment of crystal polar axes perpendicular to the substrate surface during growth and the same polarization orientation in most of the grains. The grains within the film are randomly oriented, creating a conical symmetry (∞m) that creates piezoelectric and pyroelectric effects. In contrast, ZnO ceramics with randomly distributed grains exhibit spherical symmetry ($\infty\infty$m), lacking piezoelectric and pyroelectric responses. These ceramics cannot be transformed into piezoelectric or pyroelectric materials through electric field poling, as ZnO is non-ferroelectric, and its spontaneous polarization vectors cannot be externally aligned.[10]

Polycrystalline piezoelectrics are more common than single-crystal piezoelectrics given their easier production processes and lower cost. Single crystals are naturally piezoelectric, in contrast to some piezoelectric ceramics or polymers, which must first undergo a poling process with a strong electric field above their coercive field to force the domains' polarization vectors to rearrange along the direction of the external electric field. After they are polarized, they become anisotropic.[11] In inorganic compounds, piezoelectricity arises from the relative displacement of ions, while in organic materials, from the position of molecular dipoles changes.[12]

Ceramic piezoelectric materials are characterized by higher stiffness and Curie points than piezoelectric polymers. The latter, in contrast, are flexible and have low dielectric constant and low acoustical impedance. Despite showing lower piezoresponse than ceramics, polymers have many other practical advantages such as nontoxicity, biodegradability, biocompatibility, relatively low-power consumption, and low cost.

Piezoelectric materials in general have important advantages: very fast response, high bandwidth, and high operating frequencies, high stiffness, the possibility to be used both ways—as an actuator or sensor, insusceptibility of the piezoelectric effect to environmental changes, and efficient control of small displacements with applied voltage. However, small displacements and limited strains, low material tensile strength, nonlinear response, hysteresis, and creep limit their applications.

Devices based on piezoelectric materials can also benefit from the periodic arrangement of their elements creating periodic nanostructures, photonic crystals, and metamaterials. Nanostructured materials with periodic variations in refractive index, known as photonic crystals, can control the flow of light, enabling the creation of bandgaps that selectively allow or prohibit certain wavelengths. Photonic crystals find applications in designing compact optical devices, such as filters, modulators, and waveguides, contributing to the miniaturization and efficiency of optical communication components. The idea of active control of photonic crystal bandgap with an external electric field led to the design of a photonic crystal made of alternating piezoelectric and dielectric layers. In addition, an implementation of a piezoelectric defect layer results in a structure offering a narrow, adjustable bandpass in a wide adjustable bandgap.[13] This type of structure can be applied in time-domain wavelength-division multiplexing devices in optical communication that allow for the construction of multiwavelength networks.
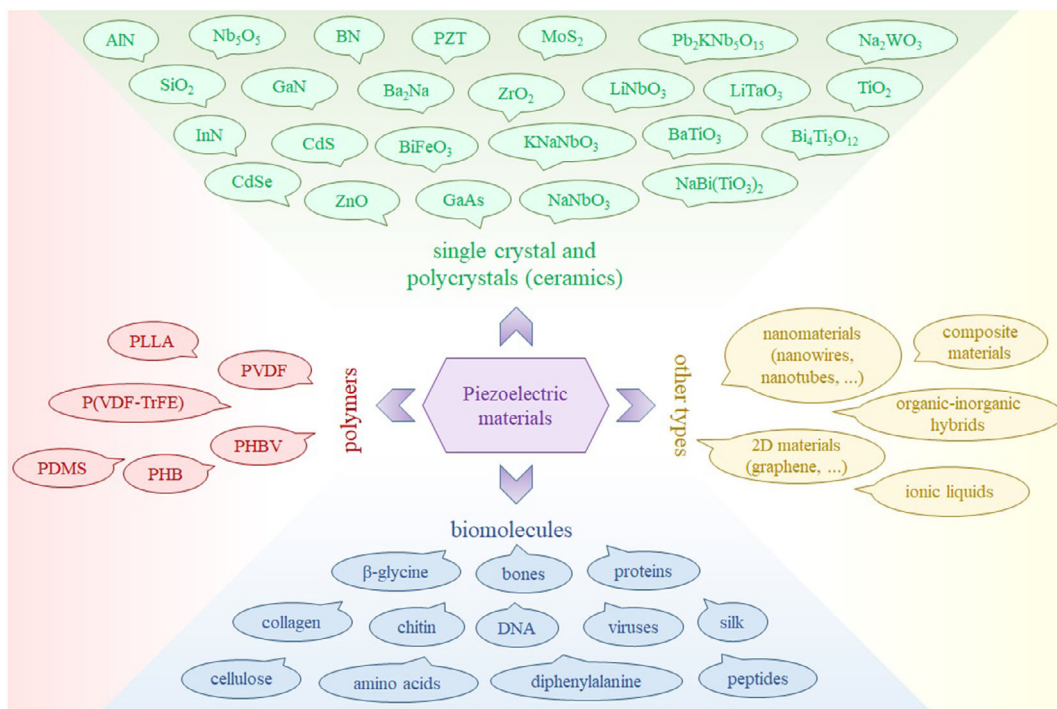
Figure 1. Examples of piezoelectric materials.

ADVANCED
SCIENCE NEWS
www.advancedsciencenews.com

physica
status
solidi
a
www.pss-a.com

Metamaterials are artificially engineered materials that can possess exotic EM, thermal, acoustic, or mechanical properties not observable in nature. Their extraordinary behavior does not come from their chemical composition but from the periodic structure of small inhomogeneities at scales much smaller than the wavelength they interact with.[14] Piezoelectrics are a powerful tool that opens up new possibilities to actively tune the optical properties of metamaterials. Piezoelectric metamaterials are typically composed of periodic arrays of piezoelectric elements, which can convert mechanical stress into electrical voltage and vice versa, which allows them to manipulate and control the wave parameters in ways that are beyond the reach of conventional materials, as negative refractive indices, leading to innovative solutions like superlenses and perfect absorbers. There are two main types of piezoelectric metamaterials: acoustic and EM. The former controls the direction, frequency, and amplitude of acoustic waves (sound or ultrasound waves). Electromagnetic piezoelectric metamaterials, in contrast, control EM waves (radio waves, microwaves, visible light). They can be used to enhance or attenuate EM waves amplitude or to manipulate their polarization and direction. Piezoelectric nanostructures find applications in designing compact optical devices, such as filters, modulators, and waveguides, contributing to the miniaturization and efficiency of optical communication components.

The piezoelectricity is intrinsically linked to the linear electro-optic Pockels effect by a shared prerequisite: a noncentrosymmetric crystal unit cell. This fundamental structural characteristic, distinguished by the absence of an inversion center, is essential for the manifestation of both phenomena and both effects occur in crystals belonging to the same point groups (see Section 2). The linear electro-optic effect encompasses the linear change in the refractive index of the optical material under the applied external electric field. Piezoelectric effects typically exhibit lower bandwidth and longer response times compared to the Pockels effect. This arises from the difference in nature of the two phenomena: the Pockels effect modulates light through an optical process, whereas piezoelectricity relies on the interplay between electrical and mechanical properties. While piezoelectricity can introduce unwanted disturbances (piezoelectric ringing) from an electro-optic perspective, the Pockels effect it induces can be beneficial for piezoelectric applications. This is particularly useful in piezoelectric optical modulators, a key component in optical communication.

Piezoelectricity can be also combined with the semiconductor properties of a material giving rise to piezotronics. Piezopotential generated by the mechanical stress or strain in piezoelectric semiconductors (like ZnO, GaN, InN) modulates the energy barrier height, which allows control of the electric charge carriers transport across the metal–semiconductor interface. The principle of piezotronics was explained in 2007 by Zhong L. Wang.[15] Piezotronics has promising applications in microelectromechanical systems (MEMS), sensors, transistors, electromechanical memories, nanorobotics, flexible devices, etc. By combining piezotronics (piezoelectric and semiconductor properties) with photoexcitation, a new effect, called piezo-phototronics, can be observed. It uses the piezoelectric potential to modulate the generation, transport, separation, and recombination of the carriers at contacts or junctions.[16] It improves the performance of optoelectronic devices, such as solar cells, light-emitting diodes (LEDs), and photodetectors. The physical foundations of piezo-phototronics were published in 2010 by Wang and coauthors.[17] However, the discussion about piezotronics and piezo-photonics is beyond the scope of this review.

In contrast, designing the new piezoelectric-based devices is expensive and time-consuming. It requires optimization and this is where a solution based on artificial intelligence (AI) can gain value. AI can analyze huge amounts of data in a finite time[18] and by performing simulations (which humans cannot do so effectively) it can identify the optimal material composition, geometry, and operating conditions to increase the efficiency of devices developed from such designed high-performance piezoelectric materials.[19] As a consequence, solutions based on AI can introduce a real revolution in the field of broadly understood materials engineering, including nanomaterials. Another field of application of AI in piezo technology could be to monitor the operation of piezoelectric devices and detect potential faults or anomalies in real time.[20] When it comes to optical communication, AI-based algorithms may also enable the seamless integration of piezoelectric-based devices with other components, which is crucial for the effectiveness of the communication system.[21]

This article reviews recent advancements in piezoelectric-based devices for optical communication. It particularly focuses on exploring potential applications through the use of AI models. Specifically, we aim to answer the following research questions (RQs): RQ1: How can piezoelectrical-based devices support optical communication? RQ2: What are the progress and research plans in developing piezoelectric-based devices suitable for optical communication? RQ3: How can AI-based algorithms be beneficial in the field of piezoelectric-based devices for optical communication? To address these RQs, a systematic review based on the PRISMA statement and its extensions[22] was conducted.

2. Basic Principle of Operation

The word piezo comes from the Greek word meaning "to press". Piezoelectricity means electricity resulting from applied pressure. Piezoelectricity is a material property strongly connected with crystal symmetries. This phenomenon occurs in materials with ionic or partly ionic bonds, whose unit cell does not possess a center of symmetry (has no inversion symmetry). Of the 32 point groups in all crystallographic systems, 21 that are noncentrosymmetric, 20 of which are piezoelectric (1, 2, m, 222, 2 mm, 4, −4, 422, 4 mm, −42 m, 3, 32, 3 m, 6, −6, 622, 6 mm, −6 m2, 23, −43 m in Hermann–Mauguin notation), with exception of 432 group (gyroid).[8] In such materials, the centers of cations and anions in the unit cell shift relative to each other when external stress or strain is applied (**Figure 2**). This shift results in an electrical dipole moment (internal electric polarization, piezoelectric polarization), which leads to the appearance of macroscopic electrical potential distribution (piezopotential) proportional to mechanical stress.

When a mechanical stress or strain is applied to a short-circuited piezoelectric material, the free charges continue to flow until the polarization effect is neutralized. In the steady state, irrespective of the presence of external stress/strain, no charge flow is observed. Both the crystallographic orientation
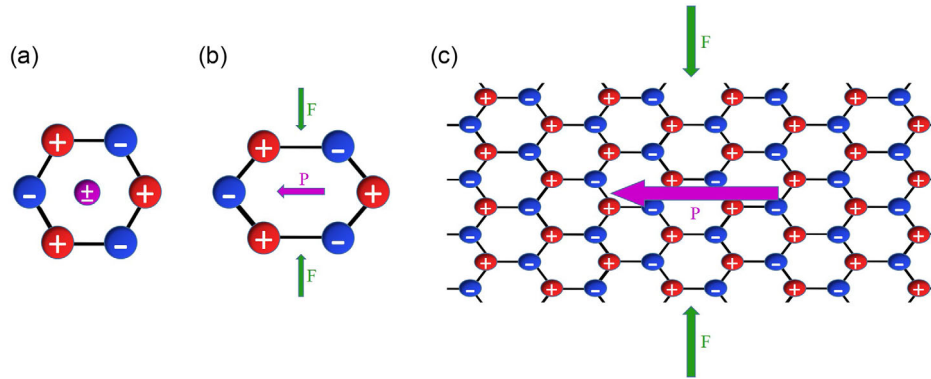
Figure 2. Mechanism of the piezoelectric effect: a) a molecule not subjected to stress shows no piezoelectric polarization, b) the molecule subjected to an external force (F) shows piezoelectric polarization (P), and c) resultant polarization of a piezoelectric material subjected to an external force.

(orientation of the cutting relative to crystallographic axes of the crystal) as well as the direction and value of the stress are important for the direction and size of the charge created on the piezoelectric plate. In case the material is compressed along the poling axis, or if it is stretched in a direction perpendicular to its polarization axis, the resulting voltage will have the same polarity as the poling field. Conversely, if the material is stretched along the poling axis, or if it is compressed in a direction perpendicular to its axis, the resulting voltage will have the opposite polarity to the poling field.[23]

Any material that exhibits the direct piezoelectric effect will also exhibit the reverse piezoelectric effect. The latter is responsible for the occurrence of mechanical deformation (expansion or contraction) of a piezoelectric material under the applied voltage. It can be used for the production of ultrasound waves.

A composite material containing two layers of different piezoelectrics bonded together (a bimorph) bends when an electric voltage is applied due to their different response to the electric voltage. This structure can be used to generate motion (actuators, pumps, speakers, precise positioning), measure force (sensors, microphones, accelerometers), or harvest energy from vibrations or footsteps.

2.1. Constitutive Relations

In this section, we will briefly discuss the mathematical description of piezoelectricity. For simplicity, we will analyze a linear range of piezoelectric properties. First, let us consider the individual effects of electrical and elastic behavior. Electric displacement induced in the insulator (separation of positive and negative charges in the material) is proportional to the applied electric field. Then, the electrical properties of the material can be described as

$$D = \varepsilon E \tag{1}$$

where D (C m^{-2}) is the electric charge density displacement, ε (F m^{-1}) is the second-order tensor of dielectric permittivity of the material, and E (V m^{-1}) is the applied electric field. The relative dielectric permittivity of the piezoelectric material ε affects its ability to store and transfer electric energy. When the

dielectric permittivity decreases, the material's efficiency in converting mechanical energy into electrical signals may be improved.

Hooke's law of elasticity combines the applied mechanical stress and strain of the material revealing that the strain (deformation) of an elastic material is proportional to the applied stress:

$$S = sT \tag{2}$$

where S (m m^{-1}) is the mechanical strain generated by the reverse piezoelectric effect, s (m^2 N^{-1}) is the fourth-order tensor of the elastic compliance, and T (N m^{-2}) is mechanical stress.

In practice, piezoelectricity can be considered as electromechanical coupling between elastic and dielectric material properties. The constitutive relations describing the coupling between mechanical stress T, mechanical strain S, electric field E, and electric displacement D can be written in four different forms:

Strain–charge form:
$$S = s_E T + d^t E$$
$$D = dT + \varepsilon_T E$$

Stress–charge form:
$$T = c_E S - e^t E$$
$$D = eS + \varepsilon_S E$$

Strain–voltage form:
$$S = s_D T + g^t D$$
$$E = -gT + \varepsilon_T^{-1} D$$

Stress–voltage form:
$$T = c_D S - q^t D$$
$$E = -qS + \varepsilon_S^{-1} D$$

$$\tag{3}$$

where c (N m^{-2}) is stiffness coefficient; d (C N^{-1}) is the piezoelectric strain–charge coefficient; e (C m^{-2}) is piezoelectric stress–charge coefficient; g (m^2 C^{-1}) is piezoelectric strain–voltage coefficient; q (N C^{-1}) is piezoelectric stress–voltage coefficient; subscripts E, T, D, S mean that the corresponding parameter is measured under no (or possibly constant) electric field, stress, electric displacement, or strain, respectively; and t means transposition.[23,24] The piezoelectric coefficient d measure the relationship between the applied mechanical stress and the direct piezoelectric effect or converse piezoelectric effect.[25,26] As the value of these coefficients increases, the performance for both sensing and actuation increases. Similarly, coefficients e, g, and q measure the relationships between the applied stress or strain and resulted charge or voltage, respectively.

The linear approach to constitutive relations has some limitations. In reality, the piezoelectric effect is nonlinear due to hysteresis and creep. The hysteresis characteristic means that there is a difference between the displacement–voltage curves for increasing and decreasing voltage. Hence, the resulting displacement of the piezoelectric material depends not only on the applied voltage but also on the history of input voltage.[27] A piezo creep is a phenomenon, where the material continues to deform even after the applied voltage has been stabilized. In addition, the dynamics of piezoelectric materials are described by the linear constitutive equations to a good approximation only for small strains and low excitation field amplitudes. For larger strains or higher fields, nonlinear effects become more significant and the linear approximation is no longer valid. Moreover, the linear constitutive relations do not account for the temperature and electric field dependence of the piezoelectric coefficients. Despite those limitations, they are relatively simple to use and are a reasonable approximation of piezoelectric properties in a range of low electric fields and small strains.

2.2. Main Parameters

Essential parameters for evaluating and understanding the performance of piezoelectric-enabled devices in optical communication include piezoelectric coefficients, dielectric constants, mechanical properties, and specific performance metrics related to optical communication devices. In addition to the piezoelectric coefficients d, e, g, and q described in Section 2.1, there is also a mechanical quality factor Q, which measures the damping of mechanical vibrations in a piezoelectric material. It is defined as

$$Q = \frac{f_r}{f_2 - f_1} \tag{4}$$

where f_r is the resonance frequency and f_1 and f_2 are frequencies at $-3\,\mathrm{dB}$ of the maximum admittance. A higher value of Q indicates lower energy loss which is important in high-frequency applications.

The parameter, that is especially important in optical communication, is the resonance frequency f_r, i.e., frequency at which the piezoelectric device naturally oscillates with maximum amplitude. In the case of negligible damping, it is equal to the characteristic frequency f_0 and can be expressed as follows:

$$f_r = \frac{1}{2\pi} \sqrt{\frac{K}{m_t + m_a}} \tag{5}$$

where K is the stiffness of the device and m_t and m_a are the inner mass of the vibrating element and the external additional mass, respectively.

The electromechanical coupling coefficient k_t is another critical parameter of a piezoelectric device since it relates the energy conversion between mechanical and electrical domains and the effective bandwidth. The lower the value, the lower the energy conversion efficiency is. For a flat unloaded resonator and vibrations along the thickness direction, it can be expressed as[28]

$$k_t^2 = \frac{\pi f_r}{2 f_a} \tan\left(\frac{\pi}{2}\left(1 - \frac{f_r}{f_a}\right)\right) \tag{6}$$

where f_a is antiresonance frequency. An effective electromechanical coupling coefficient can be defined as

$$k_{eff}^2 = (f_a^2 - f_r^2)/f_a^2 \tag{7}$$

which can be applied as an approximation to both unloaded piezoelectric block material and assembled arrays.[28]

The bandwidth BW, which is the range of frequencies over which the device can effectively operate, is related to the mechanical quality factor of the resonator. It can be written as follows:

$$BW = \frac{f_0}{Q} \tag{8}$$

Another important parameter is power consumption (i.e., amount of electrical power required for the device to operate). Lower power consumption is advantageous for energy-efficient systems.

In turn, the signal-to-noise ratio (SNR) is crucial for reliable communication.[29] The SNR of a piezoelectric sensor can be expressed as a ratio of signal power to noise power. This ratio allows to determine the clarity of the signal produced by the piezoelectric device concerning the background noise.

In the designing of optical modulators and sensors, also the strain-induced refractive index change Δn must be taken into account, that is

$$\Delta n = n_0 \cdot \frac{\Delta L}{L_0} \tag{9}$$

where n_0 is the initial refractive index, L_0 is the original length, and ΔL denotes the change in length. This index measures the change in the refractive index of the optical material caused by the strain from the piezoelectric effect.

Also, thermal stability understood as the ability of the piezoelectric material to maintain consistent performance across a range of temperatures is of high importance in practical applications. High thermal stability ensures reliable operation in varying environmental conditions.

The range of the most important parameters is shown in **Table 1**.

2.3. The Crystal Structure

Twenty piezoelectric point groups can be divided into 10 polar (pyroelectric) and 10 nonpolar groups. Polar materials exhibit a spontaneous polarization produced by an external electric field, but only in the case of some polar subgroups (called ferroelectric), this spontaneous polarization can be reversed by the external electric field. Those piezoelectrics that are not ferroelectric are called paraelectric. They do not exhibit a permanent electric dipole moment and their polarization drops to zero when the external electric field is removed.

The crystals with the strongest piezoelectric properties usually have the non-ferroelectric wurtzite structure, e.g., GaN, AlN, InN, BN, and ZnO and they constitute most of the third-generation semiconductors. The wurtzite structure consists of a hexagonal close-packed array of one type of atom with half

Table 1. Summary of parameters' ranges.

Parameter	Minimal value	References	Maximal value	References
Piezoelectric coefficient, d[a]	10 pC N^{-1}	[199,200]	1000 pC N^{-1}	[200–202]
Dielectric constant, ε[b]	10	[200,203]	5000	[204]
Mechanical quality factor, Q	10	[205]	10 000	[206]
Electromechanical coupling, k_{eff}[c]	0.1	[207]	0.8	[207]
Sensitivity[d]	0.01 V μm^{-1}	[208]	10 V μm^{-1}	[208,209]
Signal-to-noise ratio, SNR	30 dB	[29,210,211]	80 dB	[29,211]
Modulation depth, ΔV	0.1 V	[212]	100 V	[213]
Time response, t_r[e]	1 ns	[214]	1 ms	[215]
Power consumption	1 mW	[216,217]	1 W	[218]
Resonance frequency, f_r	1 kHz	[209]	10 GHz	[219,220]
Bandwidth, BW	10 kHz	[221–223]	1 GHz	[224]
Strain-induced refractive index change, Δn	0.001	[225]	0.1	[226]
Thermal stability[f]	−40 °C	[227]	150 °C	[208,227]

[a]PZT ($\approx$250–500 pC N^{-1}), PVDF ($\approx$20–30 pC N^{-1}), and lead-free ceramics like barium zirconate titanate-barium calcium titanate (BZT–BCT) ($\approx$600–800 pC N^{-1}). [b]PZT ($\approx$1000–1500), PVDF ($\approx$10–20), and barium titanate ($\approx$2000–5000). [c]PZT ($\approx$0.4–0.7), PVDF ($\approx$0.1–0.2), and lead-free piezoelectrics ($\approx$0.5–0.7). [d]High-sensitivity sensors (1–10 V μm^{-1}) and general modulators (0.01–1 V μm^{-1}). [e]High-speed modulators (1–10 ns) and general sensors (10 ns–1 ms). [f]General optical communication devices (−40–85 °C).

of the tetrahedral voids occupied by the other type.[30] In contrast, ferroelectric crystals usually have a perovskite structure, e.g.: LiNbO$_3$, PZT, i.e., Pb(Zr$_x$Ti$_{1-x}$)O$_3$, where $0 \leq x \leq 1$, BaTiO$_3$, and KNaNbO$_3$.[31] The perovskite structure is a cubic unit cell with lanthanide or alkali earth metal atoms at the cube corners, oxygen atoms at face-centered positions, and transition metal atoms in the body center.

2.4. Piezoelectric Effect in Liquids

Recently, the piezoelectric (and reverse piezoelectric) effect in liquids was demonstrated for the first time.[32] It was found in two ionic liquid salts with unsymmetrical organic cations and symmetrical weakly coordinating anions: 1-butyl-3-methylimidazolium bis(trifluoromethyl sulfonyl)imide (C$_{10}$H$_{15}$F$_6$N$_3$O$_4$S$_2$) and 1-hexyl-3-methylimidazolium bis(trifluoromethyl sulfonyl) imide (C$_{12}$H$_{19}$F$_6$N$_3$O$_4$S$_2$) at room temperature. Piezoelectricity is understood as a combination of Hooke's law of elasticity and dielectric properties of materials subjected to the electric field. However, Hooke's law (the proportionality of stress and strain for small deformations) was formulated for compressible materials. This discovery requires verification of the theory behind piezoelectricity, which, till now, has been observed only in solids with organized structures. The piezoelectricity exhibited by liquids is inconsistent with this model and reveals some extraordinary molecular organization not present in ordinary liquids. The discovery opens up possibilities for applications in electronic and mechanical systems like sensors and actuators, energy harvesting in wearable devices, optical communication, soft and fluidic robotics, dynamic focusing lenses, smart materials, self-healing materials, drug delivery, tissue engineering scaffolds, lab-on-a-chip devices, ultrasound generation, and adaptive acoustic devices.

3. Piezoelectric-Based Solutions in Optical Communication

In today's data-driven world, optical communication has emerged as an indispensable pillar of modern communication, enabling the seamless transmission of huge amounts of information over vast distances. Optical communication systems rely on a transmitter to encode information into light, a channel to transport the signal, and a receiver to extract the original message from the received light. The advantage of optical communication over radio-frequency communication is the fast and efficient transmission of large amounts of data over a long distance without significant loss.[6] This revolutionary technology harnesses the power of light to carry our digital messages, transforming the way we connect, communicate, and access information. It is based on a complex network of lasers, amplifiers, switches, and optical fibers, while FSO uses laser beams in the open air.[33] Both modalities offer distinct advantages and challenges, shaping the future of data transfer.[34,35]

Nowadays, as the demand for faster and more reliable data transmission continues to grow, researchers and engineers are exploring innovative solutions to enhance and optimize optical communication systems.[36,37] One such avenue of exploration is the integration of piezoelectric-based devices, which harness the piezoelectric effect for improved signal modulation, sensing, and control,[38] introducing a realm of possibilities to manipulate and optimize optical signals. The piezoelectric effect offers a unique set of capabilities that can revolutionize various aspects of optical communication. From modulators that enable precise control over signal characteristics to tunable filters and gratings facilitating dynamic adjustments in wavelength and bandwidth, piezoelectric technology is proving to be a transformative force.[39] Beyond modulation and tuning, these devices are also
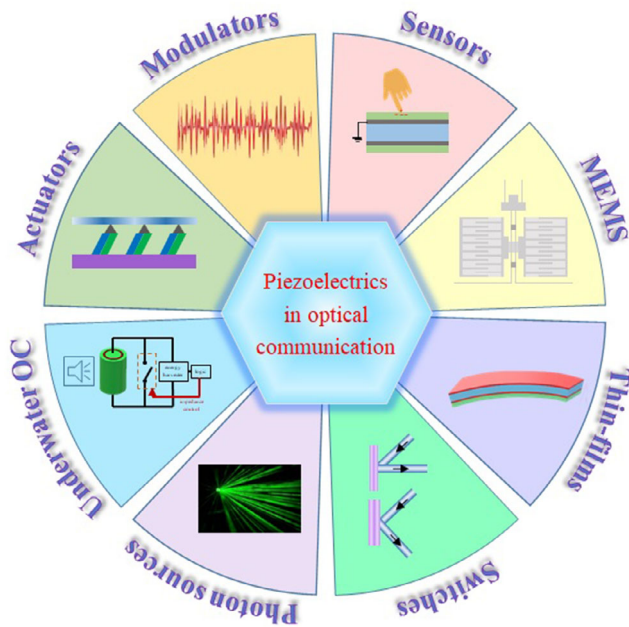
Figure 3. Piezoelectric-based solutions used in optical communication.

being harnessed for energy harvesting and environmental sensing, addressing challenges associated with power consumption and ensuring the robustness of communication networks.[40] Some of the piezoelectric-based solutions used in optical communication are presented in **Figure 3**.

3.1. Piezoelectric Sensors

In many cases, vibrations are harmful. For example, torsional vibrations of drive systems have long been the subject of research due to their importance and nuisance, as a type of mechanical vibrations naturally related to the basic rotational movement of the considered object. Eliminating or minimizing the amplitudes of these vibrations has always been accompanied by difficulties caused by the cumbersome application of control forces and torques to the rotating elements of the drive system without interfering with its basic operating motion[41,42] At the core of piezoelectric sensors lies the extraordinary property of piezoelectricity[43] that forms the basis for the operation of piezoelectric sensors, providing a bridge between mechanical perturbations and electrical signals. In the context of optical communication, these types of sensors are strategically placed within the system to capture and convert mechanical vibrations into electrical signals. The piezoelectric effect enables the sensors to detect changes in the optical environment, contributing to the dynamic adaptability of optical communication networks.[44] The main applications of piezoelectric sensors in optical communication are connected with vibration and alignment control, signal quality optimization, and development of the adaptive optical systems.[45]

Piezoelectric sensors play a crucial role in vibration and alignment control within optical communication systems. By monitoring mechanical vibrations and adjustments, these sensors ensure the precise alignment of optical components, such as lenses, mirrors, and fiber optics.[46] This capability enhances the overall stability and reliability of optical communication networks, especially in dynamic environments.[47] For example, Zheng et al.[48] proposed an analysis of the amount of piezoelectric material used, the energy consumed, and the maximum transient voltage to suppress vibrations in the context of eliminating the noise associated with them. In turn, Huang et al.[49] show the active vibration control system based on piezoelectric stack actuators. Utilizing modal transformation for vibration monitoring, an improved particle swarm optimization (PSO) algorithm to optimize strain sensor positions, and a back-propagated neutral network to implement a self-adaptive control strategy, they were able to achieve the relative root-mean-square error between estimated and measured vibration displacement less than 3%, and a vibration attenuation of over $14\,dB\,Hz^{-1}$. The sensors that are based on macrofiber composite can successfully minimize torsional vibrations.[50,51] An interesting solution for damping vibrations is combining piezoelectric elements with graphene in the form of plates to stop sound radiation.[52] A 23 dB reduction compared to the open-loop arrangement and a 12 dB enhancement relative to the velocity feedback controller was demonstrated. Another proposed compensator was based on an active–passive integrated actuator composed of a piezo-stack array.[53] It effectively isolated vibrations, achieving micro-vibration attenuation between 18% and 64%, with an isolation frequency band above 5 Hz. The key role in the case of vibration-dampening devices, apart from taking up as little space as possible, is also to consume as little energy as possible. This is also important considering the use of AI-based methods.

Piezoelectric tactile sensing is a technology that utilizes the piezoelectric effect to detect and measure touch stimuli. The mechanical stress causes the deformation of a piezoelectric material leading to a charge separation, which generates an electric field that can be measured and used to infer the magnitude, location, and type of touch stimuli. Piezoelectric tactile sensors are characterized by high sensitivity, fast response time, flexibility, and durability. In ref. [54], a tactile sensory platform for prosthetic technology was proposed. The feedback arrangement is based on a low-power optical fiber communication system and an ultra-wideband optical modulation scheme. The platform is capable of transferring data at 100 Mbps while consuming $50\,pJ\,bit^{-1}$. In ref. [55], the authors presented a self-powered flexible sensor that visualizes real-time pressure by integrating optical and electrical responses. It is composed of a microporous structure and is based on triboelectrification-induced electroluminescence with the possibility to tune colors. Rapid response time below 10 ms, high sensitivity over $190\,kPa^{-1}$ in a wide range of pressure, and the all-in-one device feature obtained by integration with a single-electrode triboelectric nanogenerator (TENG) open up a way for applications in real-time pressure mapping, and human–machine interfaces (HMI) using wireless optical communication and robotics. Another self-powered photodetector, with a 120.3 dB linear dynamic range, was shown in ref. [56]. The improved utilization of light, resulting from the reduced reflection and widened angle of the effective incident light, can be achieved with arrays of single-layer hollow ZnO hemispheres. The device is characterized by a high detectivity of 4.2×10^{12} Jones with a rise/fall time of 13/28 µs.

Ongoing research and technological advancements continue to refine the capabilities of piezoelectric sensors in optical communication. Miniaturization, integration with emerging technologies like AI, and the development of more sensitive materials contribute to expanding the functionalities of these sensors. Additionally, the exploration of new piezoelectric materials broadens the possibilities for enhanced sensor performance.

3.2. Piezoelectric MEMS/Nanoelectromechanical Systems

The basic operation principles of piezoelectric MEMS/nanoelectromechanical systems (MEMS/NEMS) resonators in the context of optical communication involve their ability to dynamically manipulate the properties of transmitted light[57–60] addressing key challenges in modulation and tuning.[61] A thorough examination of their precise control over optical signals,[62,63] particularly in terms of amplitude and phase modulation and dynamic frequency control, establishes their significance in achieving high-speed data transmission and adaptability in optical networks. This leads to facilitating advanced modulation formats and improving overall system performance,[64] enhancing the adaptability of optical networks to changing communication requirements. For example, MEMS sensors combined with optical metasurfaces provide the possibility to modulate the phase and amplitude of the reflected light.[65] Consequently, solutions enabling the manipulation of 2D wavefronts can be developed. This approach may bring benefits when implemented in reconfigurable and adaptive optical networks and systems. The 1 × 3 optical switch based on a translational MEMS platform with integrated silicon nitride (SiN) photonic waveguides was presented in ref. [66]. This device demonstrates efficient optical signal transmission between fixed and suspended movable waveguides. It is characterized by minimum and maximum average insertion loss of 4.64 and 5.83 dB, respectively, over a wavelength range of 1530–1580 nm. The average insertion loss across two air gaps was reduced even by a maximum of 7.89 dB thanks to a unique gap-closing mechanism. In optical communication, precise timing and synchronization are critical.[63] Piezoelectric MEMS resonators offer unparalleled precision in frequency control, making them ideal for applications in optical clock oscillators.

MEMS-based resonators enable selective detection of long-wave infrared radiation with high accuracy reducing the noise equivalent temperature difference of multispectral thermal imagers to ≈1 mK.[67] The application of piezoelectric MEMS resonators in optical communication enables wavelength tuning due to the possibility of integration with tunable lasers and optical filters.[68] They also enable precise optical control, stability, and tuning capabilities. As optical communication systems evolve, the role of piezoelectric MEMS resonators is anticipated to expand. Ongoing research focuses on refining their performance characteristics, exploring novel materials, and integrating them with emerging optical technologies.[69] Also, light detection and ranging (LiDAR) sensors have recently been widely applied, in particular in the field of autonomous cars due to their ability to improve the process of recognizing the vehicle's surroundings. LiDAR may contain MEMS. This approach influences compactness (smaller size of the device and simplification of the design),

allowing scanning of the environment at high speed, reaching an average resonant frequency of 1264 Hz (995 Hz) and maximum optical scan angle of 26° (44°) for two different models.[37]

Other MEMS application fields are connected with the aeroacoustics measurements, i.e., aerospace industry.[64] The materials from which MEMS/NEMS are made of aluminum nitride (AlN),[70–72] PZT,[73,74] silicon (Si),[75] carbon nanotubes,[76] and graphene.[77] Also, periodic synthetic material like cross-section connection–phononic crystal can be applied as a composite of MEMS.[78] Some solutions based on MEMS consist of the so-called green piezoelectric materials. One of these kinds of materials is zinc oxide (ZnO). Its advantages are biocompatibility, biodegradability, and low deposition temperature (which reduces the cost of sensor production).[79] This contributes to the fact that they can also be used as ultrasensitive biosensors,[80] including for mass/pressure detection in medical applications.[81] However, this kind of material may be sensitive to variations in temperatures.

The Si-based MEMS sensors are commonly implemented in gas-detection devices, which must have a low limit of detection (LOD).[60] These solutions may be applied to chemical sensors, which reached LOD of dimethyl methyl phosphonate (as a simulant of extremely toxic organophosphorus compounds) as low as 5 ppb using parylene-C-patterned microcantilevers with metal-organic framework of UiO-66 film[82] humidity sensors,[83] which showed high relative humidity (RH) sensitivity of 10.45 Hz/% RH, fast response, and recovery times of about 1 s, less than 5% stability variation and with less than 3% RH hysteresis error, or detectors of volatile organic compounds.[84] Also, their manufacturing process is quite complex, which may be disadvantageous in commercial applications. To minimize the last drawback, the integration with complementary metal–oxide–semiconductor (CMOS) was proposed.[85,86] Other advantages are connected with the monolithic integration of CMOS and MEMS on the same chip and in this way the development of compact and lightweight devices (miniaturization process).[87] Although miniaturization increases the level of performance of the sensor, it leads to the reduction of the transduction area, and consequently the low proportion of the signals to noise coefficient.[88]

Miniature transistors embedded in integrated circuits play a crucial role in optical communication, enabling functions like modulation, amplification, signal processing, switching, and routing of light information. The integration of transistors into the optical domain increased further the data rates and bandwidth in communication systems, offering the encoding of information with exceptional precision. They allowed for modulation based on amplitude, phase, or frequency, ensuring the integrity and reliability of data transmission over optical channels. However, issues such as scalability, power consumption, and compatibility with existing infrastructure require continued attention. Research is being conducted on the highly enhanced performance of integrated piezo-photo-transistors with dual inverted organic light-emitting diode gate and nanowire array channel yielding current on/off ratio of 10^6[89] or tuning stability enhancement of all-fiber acousto-optic tunable filter based on multi-piezoelectric transducer.[90] Future directions include the development of more energy-efficient transistors, advancements

**ADVANCED
SCIENCE NEWS**

www.advancedsciencenews.com

pssa
physica status solidi

www.pss-a.com

in nanophotonics, and the exploration of quantum technologies for even faster and more secure communication.

3.2.1. Piezoelectric Thin Films

In addition to standard piezoelectric crystals or ceramics, there is a growing field of piezoelectric thin films. Due to their very low volume, they are characterized by low-power consumption and compact footprints. Their integration with microelectronic circuits allows them to function as microscale sensors and actuators. This miniaturization opens doors for a new generation of MEMS with low-power consumption. Such piezoelectric films can be integrated with plasmonic, photonic, or metamaterial surfaces, leading to new functionalities and applications combining EM and mechanical properties. Due to those unique properties that distinguish thin-film technology from bulk crystals, we decided to dedicate a separate subsection devoted to thin-film piezoelectrics.

A thin-film technology can be used to reduce the power consumption of photonic integrated circuits used in optical communication, photonic quantum information processing, optical phased arrays, etc. For example, in ref. [91], a doped HfO_2 piezoelectric 20 nm thin-film actuator is used for an active ultralow-power tuning of a hybrid microring in silicon photonics. This integrated platform can perform efficient (wavelength tuning efficiency: $8.4\,pm\,V^{-1}$ and power efficiency of $0.12\,nW\,pm^{-1}$) linear bidirectional tuning with $3.07\,\mu W$ per free spectral range estimated power consumption.

An integration of piezoelectric thin film with optical elements opens new possibilities in manipulating EM radiation. For example, an active optical metasurface composed of a thin-film piezoelectric MEMS system and gap surface plasmon metasurface for dynamic, fast response (<0.4 ms) and controllable 2D broadband modulation ($\approx 20\%$ near the 800 nm wavelength) of the amplitude and phase at the subwavelength scale was proposed in ref. [92]. They presented polarization-independent reflected beam steering and reflective 2D focusing with high modulation efficiencies ($\approx 50\%$) by finely acting the MEMS mirror. The structure consists of an optical metasurface layer containing metal nanobricks and a back reflector that are physically separated by an electrically controlled air gap, with an ultra-flat MEMS mirror serving as a moveable back reflector. The ultracompact size and low-power consumption make it useful in reconfigurable and adaptive optical networks and systems. A year later, their group demonstrated[65] reflective electrically driven dynamic wave plates composed of thin-film piezoelectric MEMS mirror and plasmonic optical metasurfaces containing anisotropic meta-atoms that assure high polarization conversion efficiencies ($\approx 75\%$), broadband operation (≈ 100 nm near the 800 nm wavelength), fast response (<0.4 ms), and full-range birefringence control (completely encircling the Poincaré sphere). The complete electrical control over light polarization enables further integration and miniaturization of adaptive optical systems.

An integration of metalenses combined with piezoelectric thin films greatly facilitated fast tunable focusing achieved with compact integrated MEMS, not requiring bulk components and large voltages.[93] A movable metalens integrated with thin-film PZT MEMS offers an out-of-plane displacement of $7.2\,\mu m$ at 23 V. Such a varifocal setup can achieve effective focal length tunability of about $250\,\mu m$ at the wavelength $1.55\,\mu m$. A large aperture of a 10 mm water-immersible two-axis MEMS mirror was presented in ref. [94]. The four AlScN piezoelectric thin-film-based actuator cantilevers are driven simultaneously at resonant frequencies, different for water and air. The maximal tilting angle of the mirror reaches $\pm 5.2°$ at 246 Hz frequency and $\pm 1.9°$ at 152 Hz in air and water, respectively. A static actuation of micromirror can be realized with AlScN or AlN as well.[95] A design with footprints of $4 \times 6\,mm^2$ has a resonance frequency of 2.1 kHz and a maximum static scan angle of $55.6°$ at 220 V DC.

Figure 4 presents some of the achievements in the area of piezoelectric MEMS and piezoelectric thin films.

3.3. Piezoelectric Optical Switches

Piezoelectric optical switches operate by manipulating the path of light signals through the controlled deformation of piezoelectric materials. Typically, a piezoelectric crystal or thin film is integrated into the optical switch.[96] When an electric field is applied, the crystal deforms, inducing changes in the refractive index and altering the trajectory of the passing light. This dynamic control allows for functions such as switching, routing, and reconfiguration of optical signals.[96] The fast response time, low-power consumption, and compatibility with various wavelengths make the piezoelectric optical switches attractive for integration into optical networks.[97] They find applications in tasks ranging from routing and wavelength selection to beam steering, for example, an integrated Fabry–Perot-type leaky-wave antenna with a ground plane made of a tunable high-impedance surface, characterized by a high gain of 23 dBi with 30° beam steering at the 38 GHz band. It exhibits very low loss below 1 dB along with fast (order of ms) and continuous beam steering.[98] Their ability to rapidly adapt to changing network requirements enhances the efficiency and flexibility of optical systems. Piezoelectric optical switches are particularly useful in scenarios where real-time adjustments to signal paths are crucial, such as in dynamic network reconfigurations with phase shifters securing a continuous phase shift up to 180° between 50 and 65 GHz with losses around 1 dB for the whole frequency range.[99] The presented low-loss pixeled metasurfaces assure linear and wideband phase shifting. An interesting optical switching concept with low insertion loss (0.27–0.47 dB at 1550 nm with the cross talks from -24.8 to -66.5 dB, and from 0.13 to 0.23 dB at 1310 nm with the cross talks from -25.6 to -70.8 dB), based on a 1×5 microfluidic array integrated with double drives was presented in ref. [100]. Cavity-free all-optical switching can be realized with the use of nanowaveguides formed of $LiNbO_3$.[101] Their strong quadratic nonlinearity enables them to achieve very fast switching times (46 fs) and very low switching energies (80 fJ). Another solution, appropriate for wireless data center networks due to the lack of excessive cabling and high speed, is an integrated hybrid FSO/fiber network architecture with tunable sources and beam steering realized with a piezoelectric actuator.[102] The physical layer design is based on 8 racks, 2904 nodes, and 185 856 channels providing full-bisection bandwidth.
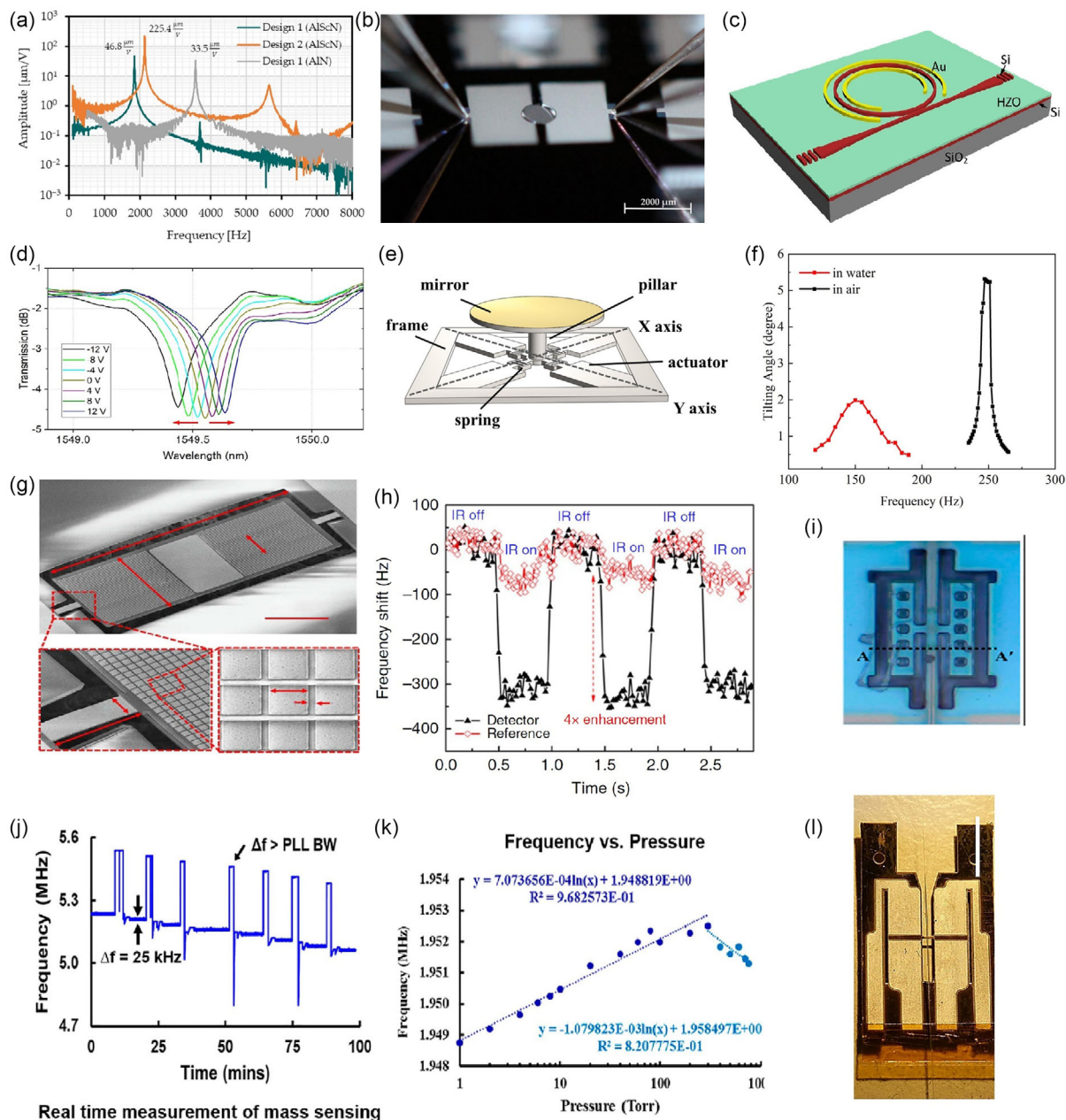
Figure 4. a) Frequency resonance functions of the presented micromirrors: mirror deflection per voltage. Reproduced with permission.[95] Copyright 2022, MDPI. b) Photography of an exemplary micromirror of Design 2 in static operation (12.5, 200 V). Captured by a single lens reflex (SLR) camera (Canon EOS 600D) and macrolens. Reproduced with permission.[95] Copyright 2022, MDPI. c) Integrated piezo-optomechanical tunable microring based on Si–HfO2 platform[91] Copyright 2023 Wiley. d) Measured transmission spectra of fabricated microring upon applying different voltages[91] Copyright 2023 Wiley. e) Structure of MEMS mirror[94] Copyright 2024 MDPI. f) Frequency responses of a thick mirror device in air and water[94] Copyright 2024 MDPI. g) Scanning electron microscopy images of the fabricated resonator, metallic anchors, and nanoplasmonic metasurface. The dimensions of the resonator are as follows: $L = 200\,\mu m$; $W = 75\,\mu m$; $W_0 = 25\,\mu m$ ($19 + 6\,\mu m$); $L_A = 20\,\mu m$; $W_A = 6.5\,\mu m$. The dimensions of the unit cell of the plasmonic metasurface are as follows: $a = 1635\,nm$; $b = 310\,nm$. IR, infrared. Reproduced with permission.[67] Copyright 2016, Nature. h) Measured response of the plasmonic piezoelectric resonator and a conventional AlN MEMS resonator to a modulated IR radiation emitted by a 1500 K globar (2–16 μm broadband spectral range). Reproduced with permission.[67] Copyright 2016, Nature. i) Optical microscope image after metal wet etching and its AA' cross section showing a trench. Reproduced with permission.[85] Copyright 2022, Frontiers Media S.A. j) II-bar thermal piezoresistive oscillator (TPO) performance evaluation for mass sensing. Real-time frequency measurements for the printing of seven Ag 1 pL droplets. The impact force causes the frequency shift to exceed the PLL bandwidth. Reproduced with permission.[85] Copyright 2022, Frontiers Media S.A. k) Resonant sensor mode. (A) Measured frequency versus pressure showing a linear in-log relationship with a turnover point at 300 Torr. Reproduced with permission.[85] Copyright 2022, Frontiers Media S.A. l) Photograph of the completed scanner; dimensions $17 \times 10\,mm$. Reproduced with permission.[73] Copyright 2024, Nature.

However, challenges such as device miniaturization, reliability concerns, and scalability issues pose ongoing research opportunities.[103] Addressing these challenges is crucial to unlocking the full potential of piezoelectric optical switches in practical applications. Advances in materials science, coupled with ongoing research into miniaturization techniques and reliability improvements, are expected to address current challenges. For example, an all-optical constellation add-drop multiplexer was proposed in ref. [104]. It is based on the constellation update and uses the quadrature phase shift keying as the minimum granularity to provide better flexibility in optical switches. Additionally, the integration of piezoelectric optical switches with emerging technologies, such as quantum communication[105] and edge computing,[106] opens new frontiers for their application.

3.4. Piezoelectric Optical Modulators

The applications of piezoelectric optical modulators span a wide spectrum within optical communication systems. They operate by harnessing the piezoelectric effect to manipulate the characteristics of transmitted light. A piezoelectric crystal or thin film is strategically placed within the optical pathway. When an electric field is applied, the piezoelectric material undergoes controlled deformation, inducing changes in the refractive index. The alteration of the refractive index modulates the phase or amplitude of the passing light, a crucial function in advanced modulation formats used for data transmission. Piezoelectric modulators facilitate the implementation of complex and precise modulation schemes, allowing for higher data rates and improved signal quality. These modulators find applications in telecommunications, fiber-optic networks, and other high-speed data transmission systems, contributing to the overall efficiency and reliability of optical communication. For example, with the improved technology of fabricating highly crystallized lanthanum-modified lead zirconate titanate thin films of high transmittance with the sol–gel method,[107] it becomes possible to effectively use a large electro-optic effect for energy-efficient optical signal modulation in an integrated optical network communication. The maximum transmittance of these thin films is 93.8% and they are characterized by an impressive quadratic Kerr coefficient of 3.54×10^{-15} m^2 V^{-2} and low insertion losses. Kohli et al.[108] presented a nanoscale high-speed (256 GB s^{-1} with a 128 GBd 4pulse amplitude modulation (PAM) signal) plasmonic Mach–Zehnder modulator based on the active electro-optic barium titanate (BaTiO$_3$) ferroelectric integrated with silicon nitride. This combination ensures a high bandwidth and low loss solution for advanced applications for the next-generation Tb s^{-1} optical interconnect platform.

One of the key advantages of piezoelectric optical modulators is their ability to effect rapid changes in optical signals in real time. This dynamic responsiveness makes them particularly valuable in scenarios where adaptive adjustments to the transmitted signal are essential. In practical terms, this capability enables compensation for signal distortions caused by external factors, ensuring a more robust and reliable communication link. The modulators can actively adapt to changing environmental conditions, making them ideal for use in diverse and unpredictable optical communication environments. A numerical analysis of an all-optical modulator composed of a layer of transparent conductive oxide Al-doped zinc oxide positioned between a distributed Bragg reflector and a dielectric metasurface made of a periodic array of cubic Si was performed in ref. [109]. The integrated device allows for tuning of the resonant wavelength of the metasurface in the C-band telecommunication window with modulation depth of 22 dB and insertion loss of 0.32 dB, which results in the possibility to change the reflection between 1% and 93%, proving to be useful for applications such as birefringence control and optical polarizer. A plasmonic metasurface formed from a lithium niobate notched-ring periodic structure coated with an electro-optical polymer demonstrates efficient optical modulation of 90 pm V^{-1} with a maximum modulation depth of 17.5 dB and an extinction ratio of 20.2 dB.[110] The changing bias voltage influences the refractive index of the polymer layer providing an electro-optical modulation scheme that can find its applications in optical signal processing, high-speed optical communication, 5G communication, and AI.

Piezoelectric optical modulators stand as a testament to the synergy between mechanical vibrations and light modulation. Their precision, adaptability, and real-time responsiveness make them invaluable in the pursuit of efficient and high-speed optical communication.

Figure 5 presents some of the achievements in the area of piezoelectric optical switches and piezoelectric optical modulators.

3.5. Piezoelectric Actuators

Piezoelectric actuators designed for optical communication, especially in space, are used in various applications, like precise optical beam stabilization in pointing, scanning, tracking, and acquisition. It can be achieved efficiently with the use of not expensive integrated miniaturized three-axis voice-coil motor actuators controlling the position of a lens.[111] The device possesses an extended field of view and can maintain the collimation and alignment of both the incident and transmitted beam, damping fluctuations caused by the atmosphere. The 24 h transmission evaluation performed on a clear weather day resulted in a 3×10^{-10} 24 h bit error rate (BER). Where the requirements for weight, size, and power for fine beam steering or fine motion mechanisms are not very strict, the piezo-stack stages can be used as a separate unit diamond-type micro-displacement amplifier.[112] However, in lightweight satellites, MEMS-based piezo actuators are a better choice. Still, the nano-positioning stages, although characterized by high resolution and precision, are capable of only minute displacement in a range of tens of micrometers. To remedy this challenge, in ref. [113] a nonresonant piezoelectric linear actuator with two motion feet was presented. This integrated device shows a resolution of 0.015 μm and a stable maximum motion speed of 17.4 mm s^{-1}. In ref. [114], a new design of the piezoelectric MEMS device based on ScAlN was proposed. Eight trapezoidal actuators arranged in the shape of the Union Flag led to the creation of an MEMS scanning mirror device with broad two-axis tilting angles and a 10 mm pupil. In the static regime, the tilting angles are $\pm 36.0°$ @ 200 V_{DC} and $\pm 35.9°$ @ 180 V_{DC} for horizontal and
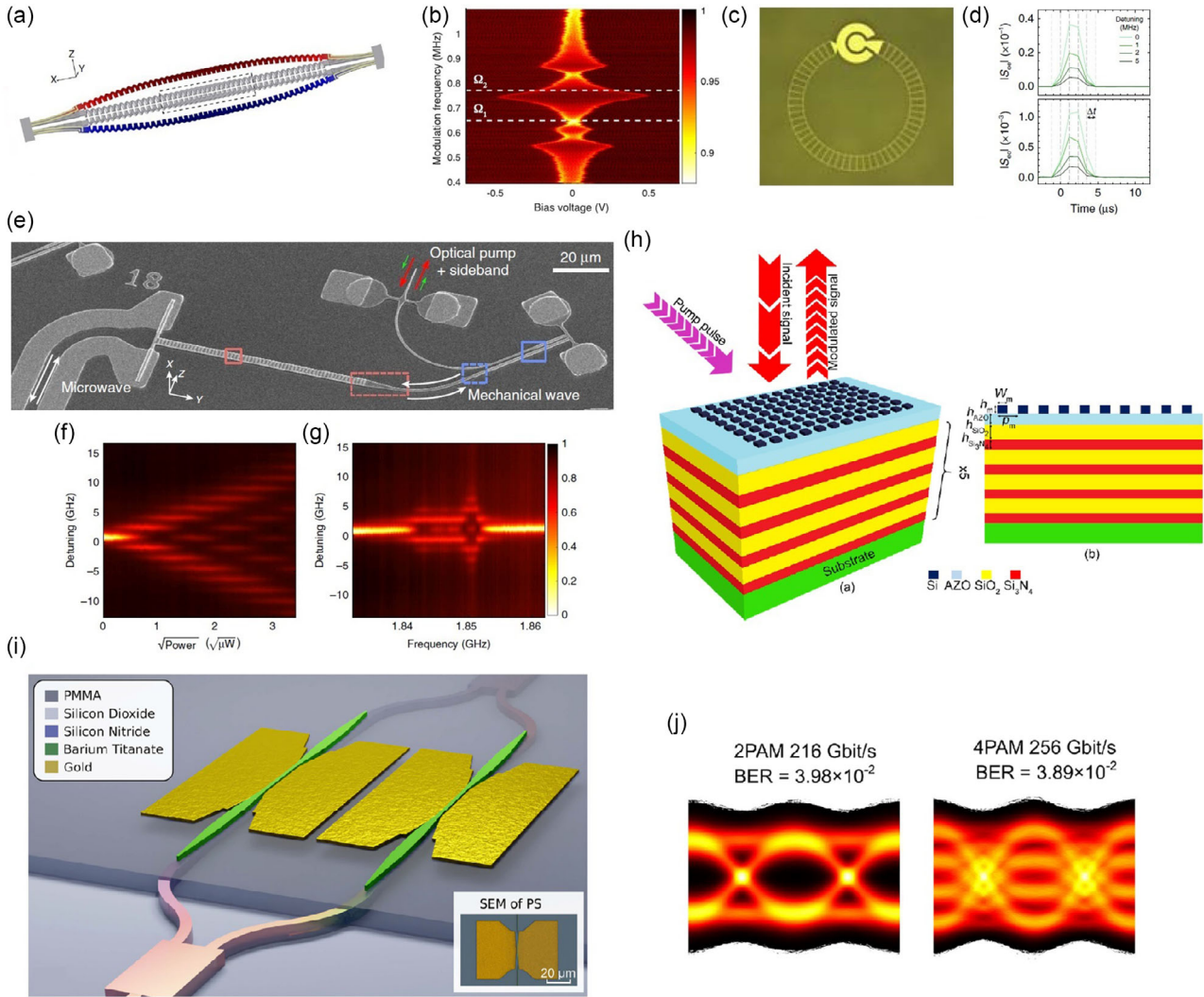
Figure 5. a) The nanobender and tunable bender–zipper cavity design. Schematic representation of how the components of the piezoelectric tensor affect the deformation of a beam (green) when a voltage is applied on electrodes (orange). Reproduced with permission.[97] Copyright 2020, Nature. b) AC modulation of a bender–zipper cavity. Measurement results for a modulation voltage of 50 mV on a bender–zipper cavity with $L = 15\,\mu m$, showing an enhanced response for certain modulation frequencies. Reproduced with permission.[97] Copyright 2020, Nature. c) An optical image of the integrated device showing the alignment between the "Ouroboros" and the microdisk. The "Ouroboros" is flipped over with its circular capacitor pad aligned above the microdisk. Reproduced with permission.[105] Copyright 2020, Nature. d) Experimental data of the pulsed conversion signals at different input detunings from the mechanical resonance ($\omega_m/2\pi = 10.220\,GHz$). The measurement time resolution is $\Delta t \approx 1.17\,\mu s$. Reproduced with permission.[105] Copyright 2020, Nature. e) Scanning electron micrographs (SEM) of one piezo-optomechanical transducer. Reproduced with permission.[103] Copyright 2020, Nature. f) Efficient acousto-optic modulation. A microwave signal sent to the interdigitated transducer (IDT) modulates the optical cavity frequency. The reflection spectrum of the optical cavity is recorded for different microwave power. Reproduced with permission.[103] Copyright 2020, Nature. g) Efficient acousto-optic modulation. The reflection spectrum of the optical cavity is recorded for different microwave frequencies. Reproduced with permission.[103] Copyright 2020, Nature. h) Schematic perspective and side view of the modulator. Reproduced with permission.[109] Copyright 2022, Nature. i) Monolithic barium titanate (BTO)-plasmonic modulator on the SiN platform. 3D illustration showing the 1:2 splitting in a SiN MMI, subsequent conversion to BTO-photonic and BTO-plasmonic waveguides, and the two BTO-plasmonic phase shifters. Inset: colorized SEM image of a reference phase shifter on the same chip. Reproduced with permission.[108] Copyright 2023, Optica Publishing Group. j) Eye diagram of the 2PAM. 216 GB s^{-1} data transmission with a BER of 3.98×10^{-2} and eye diagram of the 4PAM signal transmitting at a data rate of 256 GB s^{-1} with a BER of 3.89×10^{-2}. Reproduced with permission.[108] Copyright 2023, Optica Publishing Group.

diagonal actuations, respectively. For the dynamic actuation at 10 Hz, the orthogonal tilting angle is $\pm 8.1°/V_{pp}$ and the diagonal tilting angle is $\pm 8.9°/V_{pp}$. In ref. [115], the authors propose a gap-plasmon grating metasurface in reflection mode mounted

on a piezoelectric substrate. The distance between grating elements can be tuned using a piezoelectric mechanism. This allows a reflected beam to cover an angle of ≈3° when subjected to strain of <3.3%. And, conversely, at the same strain value, the

reflection angle is recovered with a wavelength error of ± 50 nm. The possibility to electrically tune the direction of the optical beam and to obtain a nonspecular reflection opens up applications in FSO communication and optical modulation.

However, pointing and tracking laser systems suffer also from a beam jitter which severely limits the precision and accuracy. To overcome this issue, an adaptive control scheme based on adjusting the piezoelectric fast steering mirror (FSM) to control the beam deflection angle was proposed.[116] The procedure is based on the filtered-x variable step-size normalized least mean square algorithm with two additional controllers (a proportional–integral derivative controller and a parallel adaptive controller) included in the control loop. Another proposition is based on a folded thermal actuator made up of a single silicon crystal that can tilt the 1 mm diameter mirror of about 9.4° under the voltage of 3.3 V.[117] Piezoelectric mirrors boast good steering capabilities (50 mrad) and high resolution (5 µrad), but their nonlinear and hysteretic actuation necessitates the employment of a sophisticated and bulky controller.[118] Another solution to obtain an adaptive mirror for FSO communication is precise control of many separate reflective elements arranged in an integrated high-order 349-element adaptive system.[119] The increased number of elements from 97 to 349 in the deformable mirror enabled the reduction of BER by 2–3 orders of magnitude and the increase of system servo bandwidth from 60 to 120 Hz. In contrast, instead of using a conventional Gaussian beam, a wider, flat-topped laser beam can be applied.[120] Since this kind of beam shape, unlike the Gaussian beam, features uniform intensity in a wide central area, this solution diminishes the pointing error in case of small disturbances.

Continual advancements in materials, design, and control mechanisms have propelled the evolution of piezoelectric FSMs. Miniaturization, integration with advanced control algorithms and the exploration of new piezoelectric materials are enhancing the speed, precision, and reliability of these mirrors in optical communication applications. The future of piezoelectric FSMs in optical communication holds exciting possibilities. Research directions include the integration of these mirrors in FSO communication systems,[121] their use in quantum communication networks, and advancements in adaptive optics for space-based communication. The continued synergy between piezoelectricity and optical steering is expected to shape the landscape of high-speed and adaptive optical communication.

Piezoelectric light beam deflectors harness the unique property of piezoelectric materials to deform in response to an applied electric field to control the integrated optical elements. This controlled deformation is utilized to tilt or shift optical components, allowing for the fast and precise dynamic deflection of light beams. One primary application of piezoelectric light beam deflectors is in optical signal routing. These deflectors can actively steer light beams along different paths, facilitating the establishment of dynamic and reconfigurable optical connections within communication networks. Furthermore, in LiDAR systems used for distance measurements, piezoelectric light beam deflectors play a crucial role in scanning the laser beam. This scanning capability enables LiDAR systems to rapidly and accurately measure distances, making them essential for applications

such as autonomous vehicles and environmental monitoring. An interesting arrangement of an integrated nonresonant two-axis piezoelectric laser scanner with a 7 mm mirror diameter was presented in ref. [122]. The piezoelectric actuator is based on a single-crystal $Pb(In1/2Nb1/2)O_3$–$Pb(Mg1/3Nb2/3)O_3$–$PbTiO_3$. Its possibility to achieve a wide average static mechanical deflection angle amplitude of 20.8° in two axes at a 559 Hz resonant frequency is of importance in point-to-point driving applications. However, the relatively high cost of the piezoelectric crystal used may limit the applications unless it is replaced by a more cost-effective piezo ceramics. Also, in communication networks, maintaining optimal alignment between transmitters and receivers is essential for efficient data transmission. Piezoelectric light beam deflectors actively contribute to dynamic beam alignment, compensating for misalignments caused by external factors, vibrations, or environmental changes. New research is focused on further miniaturization, increased scanning speeds, and integration with emerging technologies such as quantum communication. The adaptability of these deflectors to different wavelengths and their potential use in FSO communication systems are areas of ongoing exploration.

Traditional lenses often have fixed focal lengths, limiting their adaptability to changing communication scenarios. Multi-actuator adaptive lenses, powered by advanced materials and technologies, introduce a paradigm shift by allowing dynamic changes to the lens curvature, thus enabling rapid adjustments to the focal plane. Multi-actuator adaptive lenses leverage a combination of piezoelectric, liquid crystal, or other smart materials along with multiple actuators embedded in the lens structure. These actuators respond to electrical signals, inducing controlled deformations in the lens surface. The ability to adjust individual actuators provides fine control over the lens shape, enabling dynamic changes to the focal length. Qiao and co-authors[123] designed an adaptive lens consisting of a ten-unit piezoelectric meta surface. It enables various types of strains (additionally in a wide range of frequencies), namely generating linear movements, rotational movements, coupled modes, and large deformation values. The authors demonstrated that the piezo metasurface can generate high strains ($\varepsilon 3 = 0.76\%$), and linear motions along three axes, rotary motions around axes as well as coupled modes. It is possible to realize a broad range of focal lengths (35.82 cm $\approx \infty$) and image stabilization with significant displacements (5.05 µm along the Y axis) and tilt angles (44.02′ around the Y axis). Thus, such solutions may be beneficial in the miniaturization of devices used for dynamic focusing,[124] beam shaping and steering, and compensation for aberrations. A distinct approach to piezoelectric adaptive lenses is presented in ref. [125]. They analyze numerically and experimentally a deformation of a flexible membrane fixed in a holder with fluid underneath. The refractive power of the membrane can be adjusted by the internal fluid pressure controlled by an external voltage and temperature. It is demonstrated that the refractive power can vary from -16 to 17 m^{-1} at 25 °C and -15 to 28 m^{-1} at 75 °C. Continual advancements in materials, fabrication techniques, and control algorithms have propelled the evolution of multi-actuator adaptive lenses. MEMS technology integration, advancements in liquid-crystal technologies, and the exploration of novel materials contribute to enhancing the speed, precision,

and versatility of these lenses in optical communication applications. Future research focuses on further miniaturization, integration with emerging technologies like improvement of coupling efficiency in FSO communication with a multi-actuator adaptive lens,[126] and the development of intelligent adaptive optical systems.

Figure 6 presents some of the achievements in the area of piezoelectric actuators.
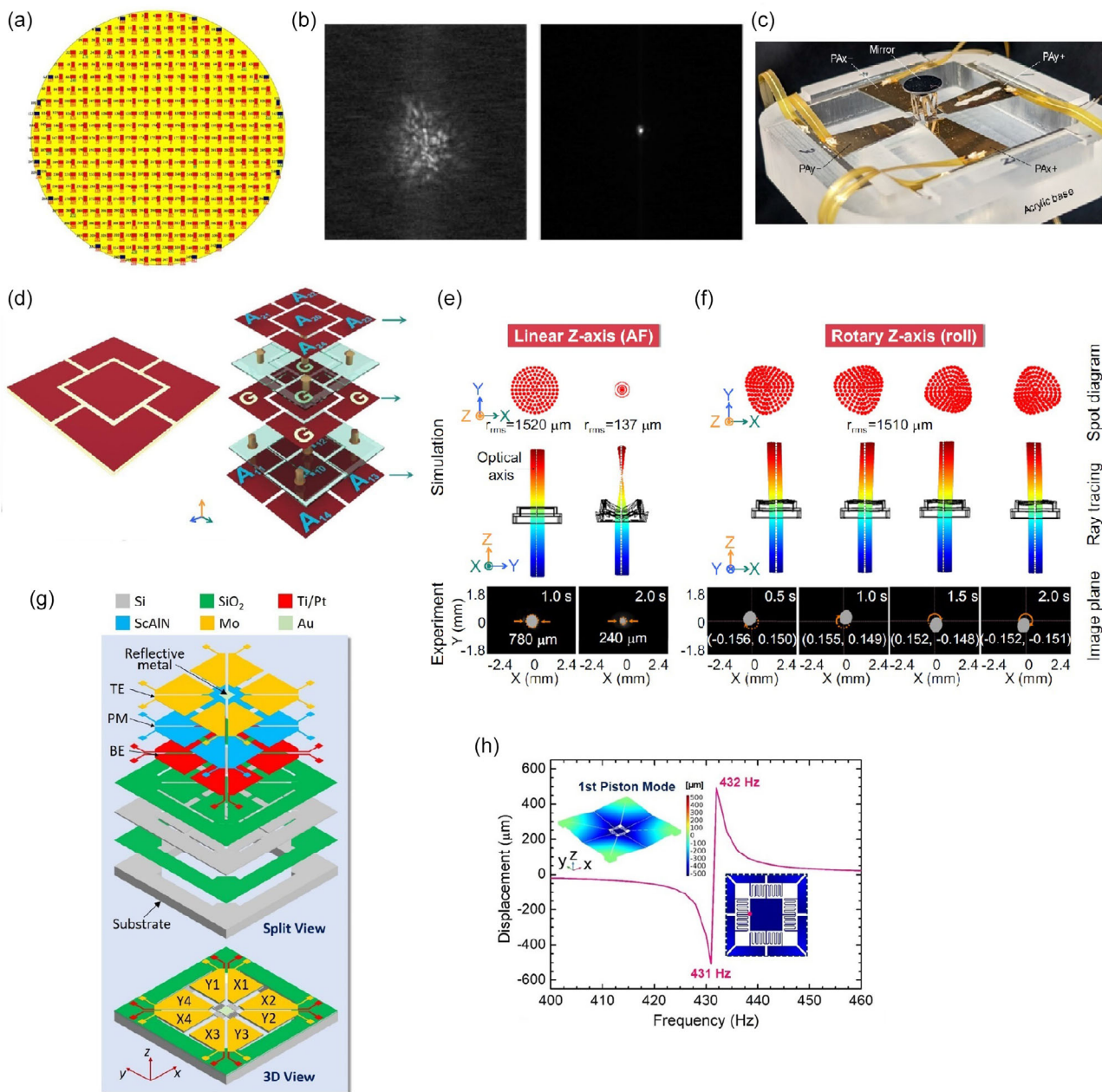
Figure 6. a) The layout of 349-element continuous surface deformable mirror (CSDM). Reproduced with permission.[119] Copyright 2019, Nature. b) Far-field image before and after compensation ($r_0 = 7$ cm) with Greenwood frequency $f_G = 17.5$ Hz. Reproduced with permission.[119] Copyright 2019, Nature. c) Photograph of the fabricated scanner. Reproduced with permission.[122] Copyright 2022, MDPI. d) Design of a piezo metasurface (PM) to generate the desired motion modes. Exploded figure of a (5 × 2)-arrayed PM. Reproduced with permission.[123] Copyright 2024, Nature. e) The PM-based adaptive lens (ALENS) based on the adjusting focus (AF) and optical image stabilization (OIS) functions under the basic modes and coupled modes for spot motion variation. Ray optics simulations (including ray tracing and spot diagram) and dynamic characteristics experiment of optical spot for AF. Reproduced with permission.[123] Copyright 2024, Nature. f) The PM-based ALENS based on the AF and OIS functions under the basic modes and coupled modes for spot motion variation. Ray optics simulations (including ray tracing and spot diagram) and dynamic characteristics experiment of optical spot for roll. Reproduced with permission.[123] Copyright 2024, Nature. g) Architectures of two ScxAl1-xN-based microelectromechanical systems (MEMS) mirrors. Reproduced with permission.[114] Copyright 2021, MDPI. h) Frequency response of Device displacement at the piston mode. Reproduced with permission.[114] Copyright 2021, MDPI.

3.6. Photon Sources

Lasing is a stimulated emission process, where a photon interacts with an excited atom or molecule, causing it to release another photon with the same energy and phase. When the process is repeated many times in a laser cavity, it results in a beam of amplified and collimated coherent light with a narrow bandwidth, finding its applications in telecommunications and medical imaging. Single/cascaded photon emission, in contrast, is a spontaneous emission process, where an excited atom or molecule randomly emits a photon, resulting in a broad bandwidth. This process can occur in any material, but it is particularly efficient in quantum dots and other semiconductors. The combination of piezoelectricity and photon sources holds great potential for advancing quantum technologies, enabling the development of more compact, efficient, and versatile sources of single and entangled photons. As these technologies mature, they are expected to play a significant role in enabling the realization of quantum computers, quantum cryptography, and advanced sensing systems.

In addition to the conventional fabrication of lasers and their control with piezoelectric transducers or actuators, there is a growing need for inexpensive and small lasers that could be integrated into on-chip devices. Lasing applications can be realized with monocrystalline $CsPbBr_3$ microwire arrays in a whispering gallery mode scheme[127] characterized by low threshold ($<3\,\mu J\,cm^{-2}$), high-quality factor (>1500), and long stability ($>2\,h$). The dynamic tuning of lasing modes is realized by a piezoelectrically induced change in the refractive index by applying strain to microwires. Lu et al.[128] showed a method of dynamically tuning the single ZnO microwire whispering-gallery mode lasing wavelength with the use of a piezoelectric effect. The dielectric constant of the wurtzite-structure ZnO microwire can be modulated with applied compressive or tensile strain (up to 0.96% and 0.94%, respectively) due to the emerging piezoelectric polarization. Significantly improved sensitivity of strain detection is of interest in laser modulation, optical communication, and optical sensing technology. Tunable single-mode lasing characteristics can be also realized in a hexagonal ZnO rod microresonator immersed in epoxy, by the combined effect of piezoelectric and piezoresistive polarization.[129] Dynamic tuning of a phase-modulating lasing mode is realized by applying external strain influencing the refractive index of ZnO. The exclusively selected single-mode lasing (modes TE_{17} and TE_{16}) can be tuned in a wavelength range 386.06–395.36 nm with a side-mode suppression ratio of 16.4 dB at a tensile strain of 0.94%. This conception paves the way for color sensors and optical switches, on-chip communication, photonic integrated circuits, and laser modulation.

A stable single and cascaded photon emission with scrutinously tuned energy is of importance in long-range fiber quantum communication at the C band. This can be achieved with the use of strain-released quantum dots made of InAs fixed on a piezoelectric substrate.[130] The device shows a long tuning range of 0.25 nm and low multiphoton emission probability (0.097), enough to overlap spectrally distant quantum dots or tuning them into resonance with quantum memories. An integrated device composed of a III–V semiconductor and a dielectric circular Bragg grating cavity attached to a piezoelectric actuator is shown to realize a single-photon source based on the Purcell effect.[131] It is possible to obtain a reversible spectral tuning of the quantum dot emitters and triggered single-photon generation with $g^{(2)}(0) = (1.5 \pm 0.05) \times 10^{-3}$. For quantum dots that are in resonance with the cavity mode, a tuning range >0.78 meV and spontaneous emission lifetimes <200 ps are achieved with an $18\,kV\,cm^{-1}$ electric field applied to the piezosubstrate. This broadband, piezo tunable single-photon emission could find applications in quantum optics, e.g., cluster states, spin–photon, and spin–spin entanglement or entangled single-photon pairs generation. A Purcell-enhanced entangled photon pair was also generated in GaAs quantum dots embedded in photonic nanostructure with quartz substrate allowing for strain transfer.[132] This source is characterized by high brightness and high entanglement fidelity of 0.88(2), and it can produce pairs of entangled photons with a pair collection probability of 0.65(4) and indistinguishabilities of 0.901(3) and 0.903(3). A single-photon emission can be also realized in strongly confined piezoelectric quantum dots made of $(211)B$ InAs/GaAs at a relatively high 230 K temperature.[133] Another possibility is to generate single photons in gated quantum dots in an open microcavity with piezoelectrically tunable emission frequency.[134] The microcavity top mirror transmission of single photons is fitted to a single-mode fiber and can be used as a single-photon source or, by manipulation of the trapped hole spin, spin–photon entangled pair creation, multiphoton cluster states creation, and single-photon transistor. It is possible to create a single photon with a probability of up to 57%, the repetition rate of 1 GHz, and with 97.5% average two-photon interference visibility. Such innovative solutions can lead, for example, to an efficient waveguide circuit construction enabling deterministic, pulsed coherent resonant single-photon creation from quantum dots built in a planar photonic nanostructure,[135] which is vital in quantum information processing.

3.7. Underwater Optical Communication

Optical communication is possible also underwater thanks to the ultra-wideband underwater backscatter (U^2B) technology using backscatter modulation,[136] i.e., the reflection of acoustic signals to transmit information. Metamaterial-inspired concentric integrated transducer containing piezoelectric materials together with algorithms that enable self-interference cancellation and frequency-division multiple-access-based medium access control provides long-range, omnidirectional, and wideband operation that allows communication at high data rates (20 kbps) at low-power consumption. Such backscatter technology finds its applications in climate change monitoring, marine life sensing, ocean exploration, underwater surveillance, and underwater communication. Another type of underwater integrated sensor is based on triboelectrification-induced electroluminescence excited by ultrasonic waves.[137] The structure consists of ZnS:Cu particles placed on a nanofibers' sheet and covered with a triboelectric layer. The advantages of this wireless, environment-friendly configuration, such as its self-powering ability, high SNR of 26.02 dB, ultrafast response below 50 ms, and very good stability with a localization of the ultrasonic source error less than

4.6% may find applications in marine sensor networks and underwater environment monitoring.

Piezoelectrics are used in underwater optical communication and also in the role of energy harvesters that use the ocean waves energy to power electrical devices. In general, a mass attached to the cantilever tip increases the mechanical deformation of the piezoelectric layer coming from the movement of the water, producing voltage across electrodes. Those energy harvesters can use, for example, wave breaking,[138] water currents,[139] or sway.[140]

Figure 7 presents some of the applications of piezoelectric in the area of photon sources and underwater optical communication.

4. AI as a Support in Piezoelectrics-Based Optical Communication

AI and machine learning (ML) are entering all areas of human life faster and bolder, offering the opportunity to significantly
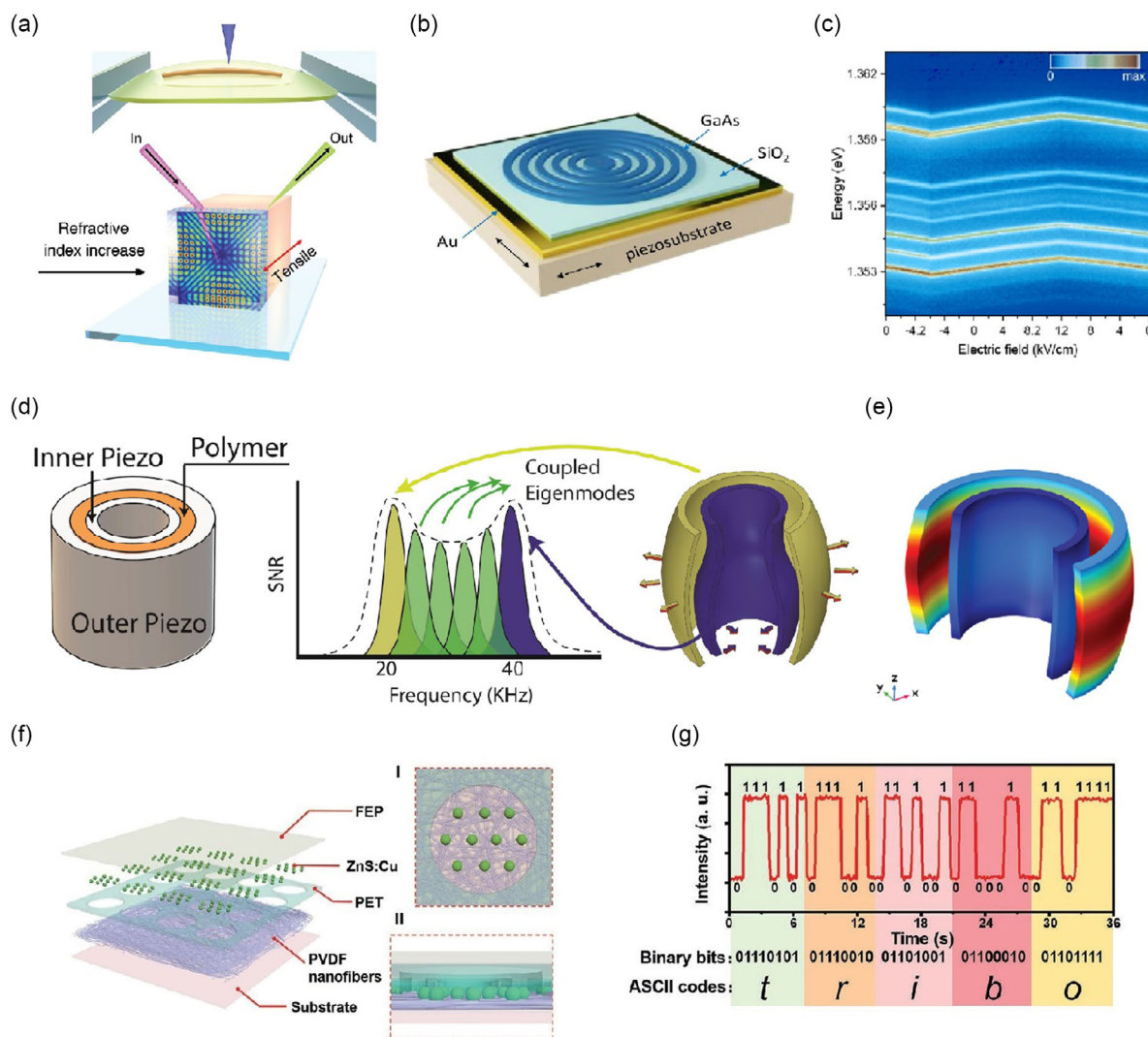
Figure 7. a) Schematic diagram showing the mechanism of tensile state. Reproduced with permission.[127] Copyright 2019, Wiley. b) Circular Bragg grating (CBG) cavity strain-tunable single-photon source. An artistic sketch of the device composed of a 125 nm GaAs membrane with In(Ga)As quantum dots (QDs), a 360 nm layer of SiO₂, and a back reflecting gold mirror bonded to the piezosubstrate. Reproduced with permission.[131] Copyright 2020, ACS Publications. c) Strain tuning of QDs emission lines embedded in the bullseye cavity. Color-coded microphotoluminescence map as a function of the applied voltage (electric field) to the piezosubstrate. Reproduced with permission.[131] Copyright 2020, ACS Publications. d) *U2B* synthesizes resonances to achieve ultra wideband (UWB) performance. The left figure shows the transducer architecture, the middle figure shows the SNR as a function of frequency, and the right figure shows one of the vibration modes—or eigenmodes—of the active layers. Reproduced with permission.[136] Copyright 2020, ACM Digital Library. e) Eigenmodes and eigenfrequencies of *U2B*'s metamaterial design. Reproduced with permission.[136] Copyright 2020, ACM Digital Library. f) Structure diagram of the self-powered all-optical wireless ultrasonic sensor (SAWS) constructed layer by layer (I: top and II: side views of one cavity unit). Reproduced with permission.[137] Copyright 2022, Wiley. g) "tribo." Reproduced with permission.[137] Copyright 2022, Wiley.

improve them. However, it brings along many challenges and ethical concerns.[141] AI enables the analysis of huge data sets ranging from medicine[142,143] to technical sciences[144] in a finite time and limits the set of considered parameters to a smaller but significant one. AI-based algorithms have also been widely adopted in optical communication.[145,146] In this context, the piezoelectrics and piezotronics supported by the AI-based solution can be applied to autonomous control, intelligent robots, and the various types of HMIs,[147,148] see **Table 2** and **3**.

Zhou and co-authors[149] proposed the sign-to-speech transition system of American Sign Language (ASL) that is based on self-powered TENG gloves, wireless transmission modules,

and ML techniques. The application of ML, namely support vector machine (SVM) enables fast gesture recognition with high accuracy (i.e., 98.63%) in less than 1 s. In turn, in ref. [150], the smart glove for virtual surgical training was presented. This approach contains triboelectric finger sensors, palm sensors, and PZT piezoelectric haptic stimulators, and the object recognition was based on both SVM and convolutional neural networks (CNNs). The application of the piezoelectrics sensors enables the design and implementation of the low-cost and low-power consumption HMI dedicated to the virtual environment that will provide tactile feedback. Not only AI-based gloves can be applied to recognize human movements, but intelligent

Table 2. The possibilities of the AI-based algorithms applications in the field of piezoelectrics.

AI-based model	Application field	References
LSTM	Prediction of muscle movement	[158]
Recurrent neural network (RNN)	Solving nonlinear piezoelectric cantilever mass–beam	[228]
CNN	Robot–manipulator	[229]
CNN	Intelligent gloves	[150,230]
CNN	Piezoelectrics socks	[152]
CNN	Prediction of the crack in composites	[165]
DNN	Intelligent cubic-designed piezoelectric node	[196]
CNN + genetic algorithms (GA)	Optimization of the geometry of the harvester	[177]
GA	Estimation of the resonator parameters	[231]
Transformer	Monitoring of the blood pressure with the wristband	[154]
SVM	Intelligent gloves fundamental parameters of thickness extensional lossy piezoelectric resonators	[150]
SVM	Robot–manipulator	[229]
RBM	Identification of the keystroke dynamic	[162]

Table 3. Piezoelectrics for optical communication concerning application fields, AI-based algorithms tasks, types, and accuracy.

Application field	Type of piezoelectrics	Type of neural network	The AI task	Accuracy [%]	References
Robot–manipulator	TENG	CNN	Classification of the shape of the objects (similar shapes and sizes)	Oval 96.1, cylindrical 97.1	[229]
Intelligent gloves	PZT/TENG	CNN	Object recognition	96.00	[150]
Intelligent gloves	TENG	SVM	ASL recognition	98.63	[232]
Intelligent gloves	PZT/TENG	SVM	Object recognition	91.00	[150]
Intelligent gloves	TENG	CNN	Sign language recognition	86.67	[230]
Intelligent keyboard	TENG	RBM	Predicting keyboard dynamics	99.40	[172]
Optimization of the geometry of the harvester	MEMS	CNN + GA	Finite element method (FEM) simulations with COMSOL Multiphysics software	90.00	[177]
Intelligent cubic-designed piezoelectric node	PZT/PEG/P(VDF–TrFE)/lactoferrin–poly(ethylene glycol) ((LF)–PEGs)	DNN	Vibration recognitions	98.00	[196]
Piezoelectrics socks	BaTiO$_3$-doped P(VDF–TrFE) fibers	CNN with multiple kernels	Classification of human activity	99.6	[152]
Skin-like optical fiber tactile (SOFT) sensor	Optical fiber tactile	Back-propagation (BP) neural network	Prediction of the parameters	92.41	[233]
Mapping of the muscle layer in the human body (movements)	PTHS	LSTM	Prediction of muscle movement	87.90	[234]
Diagnosis of fatigue hole-edge crack	Piezoelectric sensor and fiber Bragg grating sensor	CNN	Prediction of the crack in composites	86.84	[165]

socks can also be used for this purpose.[151,152] Active sensors can be also based on piezoelectric nanogenerators (PENGs), TENG, and others.[153] They may be treated as wireless sensor nodes to create a body area network. This approach combined with AI-based algorithms enables to develop of a patient monitoring network. For example, Tan and co-authors[154] used a PENG sensor with transformers in a wristband to monitor blood pressure. For this purpose, also SVM and waving-constructed self-powered pressure sensors can be considered.[155] An interesting solution based on TENG was shown by refs. [156,157], namely developing artificial skin that would enable the recognition of material textures like human fingers. The accuracy they achieved was comparable with the human tactile perception. Not only the skin but also human muscles became an object whose operation was to be reproduced by using active sensors. Fang et al.[158] proposed the reproduction of the second layer of the human body muscles. They used a piezoelectric–triboelectric hybrid self-powered sensor (PTHS) for this purpose. The movement of muscles was predicted with short-term memory neural networks (LSTM) with satisfactory accuracy (above 85.00%). Thus, signals received from such sensors can be used as input to a neural network that will then predict the user's health condition. Piezoelectrics transducers can also be used to develop eyeglass frames with a touch-sensitive surface, RimSense.[159] Touch gestures (touching the frames) generate a frequency response that serves as input to a deep neural network (DNN) predicting the user's gestures.

Sensors like TENG are among others applied to create intelligent keyboard covers,[160] or even washable and stretchable keyboards.[161] Zhao and co-authors[162] proposed to combine the AI-based algorithm and TENG in the keyboard to identify the keystroke dynamics. They used a restricted Boltzmann machine (RBM) as a classifier. Another potential application field is connected with the technology of autonomous cars. This requires advanced safety systems, which can be based on intelligent sensors.[163,164] Here, the signals that are coming from these sensors may be used as input to the AI-based model to predict the safety movement path. This invention may be potentially beneficial in the cybersecurity sector.

In contrast, the combination of AI and active sensors was applied to the evaluation of fatigue cracks in composites.[165] The input signals come from a piezoelectric sensor and fiber Bragg grating sensor (i.e., they measure the global and local response of composites). It turned out that CNN can predict cracks in carbon-fiber-reinforced polymer, commonly used in the aircraft industry, with quite high accuracy (above 85.00%). Similar results were obtained by Cosoli and co-authors.[166]

Intelligent power sensors based on piezoelectrics can be incorporated into energy-saving networks.[167–169] Tang et al.[170] proposed deep learning and TENG to develop a wireless real-time monitoring system. As a result, the system was able to predict the LED blink frequency. Zazzi et al.[171] applied an AI model in on-chip optical–electrical–optical artificial neural networks (ANN).

AI-based model in the field of piezoelectrics in optical communication is a virtual store.[114] The proposed solution combines TENG, PVDF pyroelectric temperature sensor, digital twin technology, and ML, namely an intelligent soft robot (i.e., a tri-finger pneumatic gripper). This manipulator enables the automatic grasping of objects. The TENG sensor was used in the contact area, determining the position of the object and detecting the bending angle. The users can experience the virtual shop (the physical simulation of the real space) and, at the same time, manipulate the objects/products in the real shop. Moreover, the users achieve real-time prediction based on the sensor responses. Also, the signals from the sensors are applied to the reconstruction of the scene in the virtual environment. Another potential AI application field is connected with speech recognition sensors.[172]

Another issue connected with AI and piezoelectric is property prediction. For example, in ref. [173], ANNs were adopted for the prediction of relation and values of the process parameters in the case of the electrospun P(VDF–TrFE) nanogenerator. It turned out that the predictions were highly consistent with the
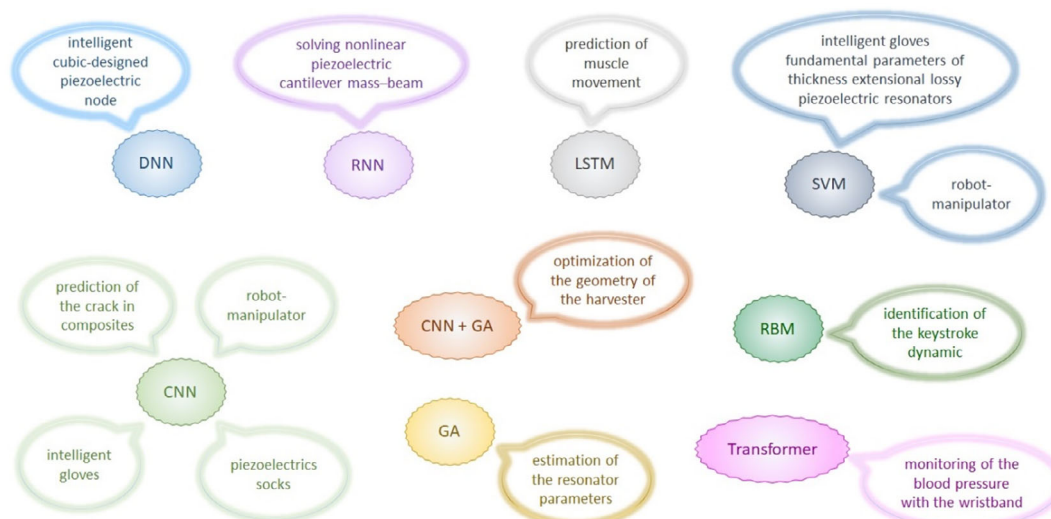
Figure 8. The possible applications of the AI-based algorithms in the field of piezoelectrics.

experimental study (i.e., error of 5%). The other potential application of AI is connected with energy harvesting.[174–176] For example, DNNs were applied to predict the optimal parameters of piezoelectric MEMS vibration energy harvester.[177] In the next step, the genetic algorithms were used to optimize the geometry of the harvester. As a consequence, the device's operational frequency was reduced by about 35%. Bhosale and co-authors[178] proposed deep belief network-based salp swarm optimization to predict piezoelectric performance. AI-based algorithms like PSO can also be applied to the optimization of the strain sensor positions.[80]

The possibilities of the AI-based algorithms applications in the field of piezoelectrics are presented in Table 2 and **Figure 8**. In Table 3, the comparison of piezoelectric and AI/ML-based techniques has been shown. It turned out that the most commonly combined with piezoelectrics neural network is CNN, however, SVM provides the accuracy of results at a similar level.

5. Discussion and Conclusions

As optical communication technologies evolve, the role of piezoelectric sensors is poised to expand further. Future perspectives include the integration of piezoelectric sensors in quantum communication systems, the development of intelligent adaptive optics, and their application in emerging technologies like FSO communication.[179] The continued synergy between piezoelectricity and optics holds promise for unlocking new dimensions in the reliability and efficiency of optical communication networks. In contrast, one can observe the rapid development of piezoelectric materials for flexible and wearable electronics, including smartwatches and smart bands.[180] For this type of solution, miniaturization is important, i.e., development of the high-quality microscale piezoelectric thin-film materials for MEMS applications. Also, wireless miniaturized medical implants have the potential to revolutionize healthcare by enabling new forms of diagnosis, treatment, and prevention. They gain much interest since they allow for continuous monitoring of patient health without the need for frequent checkups providing real-time feedback to doctors. In addition, they can be used to deliver targeted therapies or to improve patient quality of life by reducing the need for invasive procedures. To establish an efficient connection with the device, a CMOS-compatible, high-Q piezoelectric electro-optic modulator based on AlN thin-film enclosed between two Bragg mirrors was presented.[181] These have applications in solutions developed as an answer to the increasing demand for higher data rates in optical communication networks, where an important issue is the development of piezoelectric modulators that enable ultrafast modulation to support emerging communication standards and technologies.[182] For example, high-speed piezoelectric modulators are capable of modulating optical signals at multi-gigahertz frequencies.[183] Another observed tendency is to minimize energy consumption and extend the battery life of mobile devices through the application of low-power modulation techniques, energy-saving drive electronics, and voltage-controlled devices.

Another issue is connected with the development of environmentally friendly solutions. There is a growing tendency to avoid the use of lead-based piezoelectrics due to the toxicity of Pb.

Since PZT-based structures frequently have better performance than lead-free piezoelectrics it remains a challenge to switch entirely to lead-free piezoelectrics. For example, there is a need for ferroelectrics with strong piezoelectric properties showing high transparency for acoustic-optical electrical coupling applications. One of the proposed solutions is the fine-grain potassium sodium niobate–barium sodium niobate ceramics with amplified local inhomogeneity achieved by tailoring the phase and domain structures.[184] This type of lead-free ceramics is characterized by high piezoelectric and electro-optical effects, good transparency, and high Curie temperature.

There is a constant need for novel materials with tailored properties that match the more and more demanding applications. Designing topological and geometrical structures based on condensed matter physics, including symmetry principle, finite-element idea, and multiphysics coupling effects leads to the creation of a novel class of electromechanical macroscopic metamaterials in which the finite *meta*-atoms introduce artificial anisotropy.[185] Natural piezoelectric ceramics have only five nonzero elements in the piezoelectric matrix, which restricts the possible designs of piezoelectric devices. However, adding an artificial anisotropy inspired by quasi-symmetry breaking in metamaterial design allows for tuning all the zero-valued elements in the piezoelectric matrix. Moreover, nonzero artificial coefficients can be introduced, in addition to polycrystalline materials, also in amorphous materials or crystals. Another method of overcoming the constraints of piezoelectric coefficients' values imposed by the intrinsic crystal structure of the constituent material is based on the manipulation of electric displacement maps from families of structural cell patterns.[186] By additively manufacturing (3D printing) free-form, perovskite-based piezoelectric nanocomposites with complex 3D architectures, it is possible to tailor piezoelectric properties beyond the constraints of piezoelectric monolithic and foam structures. It allows for the design of arbitrary piezoelectric tensors, including symmetry conforming and breaking features, which enables tuning the resulting voltage response of the material and expanding the range of piezoelectric functionalities. This may be applied in the construction of wideband-tunable filters that enable a high level of selectivity during the filtering of the optical signals in wavelength-division multiplexing systems.[187]

Materials like PZT and PVDF are frequently applied in piezoelectric-enabled devices due to their excellent piezoelectric coefficients, advantageous dielectric properties, and strong mechanical characteristics. They are integral to the structure and function of devices like modulators, sensors, and switches, where they convert mechanical stress into electrical signals and vice versa. The core working principle involves applying strain to optical waveguides through the piezoelectric effect, which in turn modulates optical signals. Thus, the crucial performance metrics for these devices include sensitivity and responsivity, bandwidth and speed, SNR, and power consumption. Sensitivity and responsivity are crucial for a device's ability to detect and respond to mechanical stress. Bandwidth and speed are essential for the efficiency of high-speed optical communication systems. A high SNR is necessary for clear signal transmission, and low-power consumption is important for energy-efficient communication systems. Piezoelectric-enabled devices are characterized by high sensitivity to mechanical stress, which is very beneficial

when used as sensors. Another advantage is the low-power requirement and compactness, which is important in communication systems. The limitations of these materials include temperature stability, aging effects, and material fatigue.[188,189] Consequently, this translates into manufacturing challenges that arise when integrating piezoelectric materials with other optical components. However, compatibility difficulties between the piezoelectric material and the substrates used in optical circuits may lead to difficulties in achieving seamless integration. For example, PZT and PVDF age and exhibit fatigue problems. Overtime, this can contribute to degraded device performance and reliability, especially in environments with fluctuating temperatures or harsh conditions. In the context of environmental protection and care for human health, lead, which is a component of many piezoelectric-enabled devices, also raises concerns as a potentially harmful material. This creates a need for lead-free alternatives that may not yet match the properties of traditional materials.[190,191] One of the possibilities are organic piezoelectric materials, which, due to their biocompatibility, could be widely used in medicine.[192] All this leads to inherent compromises in the performance of communication systems. Addressing these limitations requires ongoing research and development to enhance material properties, improve manufacturing techniques, and design more robust and adaptable devices.

AI has a huge potential to improve the performance, efficiency, and functionality of the piezoelectric-based devices that are applied in the field of optical communication. It can provide a numerical tool to optimize the design parameters of piezoelectric devices by optimizing various material properties, geometries, and operating conditions.[193] AI may help with the identification of promising piezoelectric materials for specific optical communications applications.[194] Consequently, it accelerates the development of high-performance materials suitable for piezoelectric devices. Also, AI may support adaptive control and calibration of the piezoelectric-based devices enabling their operating parameters to be dynamically adjusted in real time to optimize performance and compensate for environmental changes or aging effects.[195] Another AI application field connected with optical communication is the development of correction algorithms to provide the minimization (or even mitigation) of signal degradation as well as to increase the efficiency of data.[196] AI in optical communication networks can also be applied as a tool to predict faults before they occur.[197] Moreover, AI-based solutions may dynamically adapt modulation formats and coding schemes in optical communication systems taking into account changing network conditions and traffic requirements.[198]

In conclusion, recent progress in piezoelectric-based devices that are designed for optical communication includes advancements in speed, tunability, integration, nonlinear effects, energy efficiency, and AI-driven optimization and control. Thus, the next generation of optical communication systems provide solutions ensuring increased efficiency, flexibility, and functionality (even multifunctionality) taking into account minimizing size and ensuring the most favorable energy balance.

In summary, piezoelectric-enabled devices have significantly advanced the capabilities and potential of optical communication, making them more practical and effective for a wide range of applications. The piezoelectric modulators and switches have enhanced the performance and speed of optical networks, meeting the increasing need for high-bandwidth data transmission. Another significant improvement is connected with health issues, namely lead-free piezoelectric materials have been engineered to provide comparable performance to traditional PZT. Thus, these key improvements include advancements in material performance, enhanced device integration, high-performance modulators and sensors, improved energy efficiency, and scalable fabrication techniques. Moreover, the combination of piezoelectric materials with other advanced materials, such as silicon photonics, has led to the development of hybrid devices. As a consequence, this procedure led to an increase in the functionality of devices based on them.

6. Future Research Lines

An important direction in the development of piezoelectric-based devices in the context of optical communication is their miniaturization and integration with other system elements to achieve minimization of the total area and reduce energy consumption. However, these issues must be related to the development of the solution that enables increasing the efficiency of the overall optical communications system, namely ensuring higher data rates, improved SNRs, and increased spectral efficiency. Another issue worth developing is the design of tunable and reconfigurable piezoelectric-based devices that would enable dynamic adjustment of device parameters, including wavelength, bandwidth, and modulation format. This would contribute to effective adaptation to dynamically changing communication requirements and network conditions. It is also worth taking into account the impact of high temperatures and other difficult conditions on communication systems during the designing of piezoelectrics-based devices. Thus, maintaining stable performance over a wide range of temperatures is crucial for the majority of outdoor communication systems and aerospace platforms. There is also growing interest in developing multifunctional piezoelectric devices capable of performing multiple optical functions simultaneously. Also, the development of intelligent adaptive optics based on piezoelectrics can pave the way for breakthroughs in emerging technologies like FSO communication. In addition, following the trend related to the green revolution, there is a need to develop other efficient piezoelectric materials than those based on toxic substances, especially lead. Also, the integration with other technologies within optical communication is of high importance, for example, connections with quantum communication or AI taking into account the process of design, optimization, adaptive control, and calibration as well as intelligent systems that diagnose and repair faults. In turn, the integration of AI with piezoelectric technology opens another direction of research, namely, developing AI models that will enable increasing the efficiency and capacity of the optical communication system in the context of improving signal detection, demodulation, equalization, and error correction.

Conflict of Interest

The authors declare no conflict of interest.

Author Contributions

Keywords

[1] J. Curie, P. Curie, *Bull. Soc. Minéralogique Fr.* **1880**, *3*, 90.
[2] Y. Zhang, W. Jie, P. Chen, W. Liu, J. Hao, *Adv. Mater.* **2018**, *30*, 1707007.
[3] Z. Yao, J. Deng, L. Li, *Matter* **2024**, *7*, 855.
[4] P. A. Villa-Machado, F. A. Restrepo-Restrepo, S. I. Tobón-Arroyave, *Int. Endod. J.* **2024**, *57*, 490.
[5] E. Donati, G. Valle, *Nat. Commun.* **2024**, *15*, 556.
[6] M. Garlinska, A. Pregowska, K. Masztalerz, M. Osial, *Future Internet* **2020**, *12*, 179.
[7] A. O. Hero, *Optical Transmission*, Encyclopedia Britannica **2024**. https://www.britannica.com/topic/telecommunications-media/Optical-transmission.
[8] J. Tichý, J. Erhart, E. Kittinger, J. Privratska, *Fundamentals of Piezoelectric Sensorics: Mechanical, Dielectric, and Thermodynamical Properties of Piezoelectric Materials*, Springer Science & Business Media, Berlin **2010**.
[9] Q. Xu, X. Gao, S. Zhao, Y.-N. Liu, D. Zhang, K. Zhou, H. Khanbareh, W. Chen, Y. Zhang, C. Bowen, *Adv. Mater.* **2021**, *33*, 2008452.
[10] D. Damjanovic, *Rep. Prog. Phys.* **1998**, *61*, 1267.
[11] R. S. Dahiya, M. Valle, *Robotic Tactile Sensing: Technologies and System*, Vol. 9789400705791, Springer Netherlands, Dordrecht **2014**.
[12] M. T. Chorsi, E. J. Curry, H. T. Chorsi, R. Das, J. Baroody, P. K. Purohit, H. Ilies, T. D. Nguyen, *Adv. Mater.* **2019**, *31*, 1802084.
[13] A. S. Firouzjaei, D. Kalhor, M. Shojaeifar, H. Goudarzi, *Optik* **2023**, *288*, 171248.
[14] A. Valipour, M. H. Kargozarfard, M. Rakhshi, A. Yaghootian, H. M. Sedighi, *Proc. Inst. Mech. Eng., Part L* **2021**, *236*, 2171.
[15] Z. L. Wang, *Adv. Mater.* **2007**, *19*, 889.
[16] C. Pan, J. Zhai, Z. L. Wang, *Chem. Rev.* **2019**, *119*, 9303.
[17] Z. L. Wang, *Nano Today* **2010**, *5*, 540.
[18] A. Pregowska, A. Roszkiewicz, M. Osial, M. Giersig, *Microsc. Res. Tech.* **2024**, *2024*, 1.
[19] J. Hu, Y. Song, *Chem. Phys. Lett.* **2022**, *791*, 139359.
[20] G. Tripathi, H. Anowarul, K. Agarwal, D. K. Prasad, *Sensors* **2019**, *19*, 4216.
[21] A. Choudhury, S. Elkefi, *Front. Digital Health* **2022**, *4*, 966174.
[22] M. L. Rethlefsen, S. Kirtley, S. Waffenschmidt, A. P. Ayala, D. Moher, M. J. Page, J. B. Koffel, *Syst. Rev.* **2021**, *10*, 1.
[23] M. V. Ravinder, S. Dahiya, *Robotic Tactile Sensing*, 1st ed., Springer Dordrecht, Dordrecht **2012**.
[24] A. Arnau, D. Soares, in *Piezoelectric Transducers and Applications* (Ed: A. A. Vives), Springer Berlin Heidelberg, Berlin **2008**, pp. 1–38.
[25] L. Chen, H. Li, Y. Guo, P. Chen, E. Atroshchenko, H. Lian, *Eng. Comput.* **2024**, *40*, 257.
[26] H. Tian, J. Liu, T. J. Kippenberg, S. A. Bhave, arXiv preprint arXiv:2405.08836, **2024**.
[27] H. Li, Y. Xu, M. Shao, L. Guo, D. An, *IOP Conf. Ser.: Mater. Sci. Eng.* **2018**, *399*, 012031.
[28] D. N. Stephens, R. Wodnicki, R. Chen, L. M. Liang, Q. Zhou, K. Morrison, K. W. Ferrara, *Ultrasonics* **2021**, *109*, 106258.
[29] Y. George, A. Sarkar, A. Javed, *e-Prime - Adv. Electr. Eng. Electron. Energy* **2024**, *7*, 100484.
[30] R. J. Lad, *Handbook of Surface Science*. Elsevier, Amsterdam *1*, **1996**.
[31] A. Cafarelli, A. Marino, L. Vannozzi, J. Puigmartí-Luis, S. Pané, G. Ciofani, L. Ricotti, *ACS Nano* **2021**, *15*, 11066.
[32] M. I. Hossain, G. J. Blanchard, *J. Phys. Chem. Lett.* **2023**, *14*, 2731.
[33] J. Wang, J. Li, D. Chen, Y. Dong, H. Ding, D. Gao, *Opt. Commun.* **2024**, *557*, 130271.
[34] M. Garlinska, M. Osial, K. Proniewska, A. Pregowska, *Electronics* **2023**, *12*, 1550.
[35] S. M. El-Garhy, A. A. M. Khalaf, M. Abaza, M. H. Aly, *Opt. Quantum Electron.* **2024**, *56*, 247.
[36] S. Gao, L. Wang, J. Lu, S. Zhang, H. Sun, K. Huang, J. Xu, Y. Hao, *IET Nanodielectr.* **2024**, *7*, 1.
[37] H. Yoon, S. Ju, C. H. Ji, *Sens. Actuators, A* **2024**, *366*, 114931.
[38] L. E. Shlapakova, M. A. Surmeneva, A. L. Kholkin, R. A. Surmenev, *Mater. Today Bio* **2024**, *25*, 100950.
[39] J. Yuan, X. Li, Q. Zhang, J. Zhang, S. Li, *Opt. Switching Networking* **2024**, *51*, 100764.
[40] Z. Li, J. Shi, N. Chi, *Neuromorphic Photonic Devices and Applications*, Elsevier, Amsterdam **2024**, pp. 319–349.
[41] B. Dyniewicz, A. Pręgowska, C. I. Bajer, *Mech. Syst. Signal Process.* **2014**, *43*, 90.
[42] J. Noh, P. Kim, Y. J. Yoon, *J. Sound Vib.* **2024**, *570*, 118004.
[43] B. Upendra, B. Panigrahi, K. Singh, G. R. Sabareesh, *J. Intell. Mater. Syst. Struct.* **2024**, *35*, 129.
[44] C. Yang, Z. Wei, H. Gao, C. H. Heng, Y. Zheng, *IEEE Nanotechnol. Mag.* **2024**, *18*, 34.
[45] S. M. Sawde, R. R. Patil, S. V. Moharil, *AIP Conf. Proc.* **2024**, *2974*, 020027.
[46] S. Arnon, N. S. Kopeika, *Proc. IEEE* **1997**, *85*, 1646.
[47] T. Liu, C. Liu, Z. Zhang, *Mech. Syst. Signal Process.* **2024**, *206*, 110876.
[48] H. Zheng, G. Zhao, W. Han, Y. Yu, W. Chen, *Struct. Multidiscip. Optim.* **2023**, *67*, 1.
[49] Y. Huang, X. Shen, B. Wang, L. Zhang, *J. Intell. Mater. Syst. Struct.* **2024**, *35*, 68.
[50] Y. Guo, Y. Yu, L. Li, D. Zhang, W. H. Liao, C. Du, X. Guo, *Compos. Struct.* **2024**, *331*, 117907.
[51] B. Wang, G. Huangfu, J. Wang, S. Zhang, Y. Guo, *J. Materiomics* **2024**, *10*, 78.
[52] H. Keshavarzpour, A. Ghasemi, *Appl. Math. Model* **2024**, *127*, 655.
[53] C. Wang, Q. Lu, K. Zhang, L. Shao, *Proc. Inst. Mech. Eng., Part C* **2023**, *237*, 799.
[54] G. Di Patrizio Stanchieri, M. Saleh, A. De Marcellis, A. Ibrahim, M. Faccio, M. Valle, E. Palange, *Electronics* **2023**, *12*, 627.
[55] L. Su, Z. Jiang, Z. Tian, H. Wang, H. Wang, Y. Zi, *Nano Energy* **2021**, *79*, 105431.
[56] X. Pan, J. Zhang, H. Zhou, R. Liu, D. Wu, R. Wang, L. Shen, L. Tao, J. Zhang, H. Wang, *Nano-Micro Lett.* **2021**, *13*, 1.
[57] M. C. Wu, O. Solgaard, J. E. Ford, *J. Lightwave Technol.* **2006**, *24*, 4433.
[58] L. Wei, X. Kuai, Y. Bao, J. Wei, L. Yang, P. Song, M. Zhang, F. Yang, X. Wang, *Micromachines* **2021**, *12*, 724.
[59] X. Le, Q. Shi, P. Vachon, E. J. Ng, C. Lee, *J. Micromech. Microeng.* **2022**, *32*, 014005.

ADVANCED
SCIENCE NEWS
www.advancedsciencenews.com

pss a
physica status solidi
www.pss-a.com

[60] S. Mariani, Z. Torkashvand, F. Shayeganfar, A. Ramazani, *Micromachines* **2024**, *15*, 175.

[61] X. Zhang, Z. Cui, H. Wu, J. Luo, T. Ye, X. Shan, T. Xie, B. Ma, *Compos. Struct.* **2024**, *329*, 117798.

[62] G. Pillai, S.-S. Li, *IEEE Sens. J.* **2021**, *21*, 12589.

[63] G. Pillai, S.-S. Li, *Sci. Rep.* **2021**, *11*, 10898.

[64] W. R. Ali, M. Prasad, *IEEE Sens. J.* **2021**, *21*, 27352.

[65] C. Meng, P. C. V. Thrane, F. Ding, S. I. Bozhevolnyi, *Nat. Commun.* **2022**, *13*, 2071.

[66] S. Sharma, N. Kohli, J. Brière, F. Nabki, M. Ménard, *Opt. Express* **2022**, *30*, 22200.

[67] Y. Hui, J. Sebastian Gomez-Diaz, Z. Qian, A. Alù, M. Rinaldi, *Nat. Commun.* **2016**, *7*, 11249.

[68] J. C. Greenwood, in *IEE Colloquium on Measurement Using Resonant Sensing*, London **1993**, pp. 1/1–1/2.

[69] Y. Hou, M. Zhang, G. Han, C. Si, Y. Zhao, J. Ning, *J. Semicond.* **2016**, *37*, 101001.

[70] F. Patocka, C. Schneidhofer, N. Dörr, M. Schneider, U. Schmid, *Sens. Actuators, A* **2020**, *315*, 112290.

[71] D. Yang, L. Yang, X. Chen, M. Qu, K. Zhu, H. Ding, D. Li, Y. Bai, J. Ling, J. Xu, J. Xie, *Sens. Actuators, A* **2021**, *318*, 112493.

[72] K. Bespalova, G. Ross, S. Suihkonen, M. Paulasto-Kröckel, *Adv. Electron. Mater.* **2024**, *10*, 2300628.

[73] W.-C. Wang, M.-Y. Li, K.-C. Peng, Y.-F. Hsu, B. Estroff, P.-Y. Yen, D. Schipf, W.-J. Wu, *Microsyst. Nanoeng.* **2024**, *10*, 13.

[74] M. M. I. Tusher, H. Lee, S. Lee, K. Lee, *Sens. Actuators, A* **2024**, *366*, 114934.

[75] G. Verma, K. Mondal, A. Gupta, *Microelectron. J.* **2021**, *118*, 105210.

[76] S. Li, X. Feng, H. Liu, K. Wang, Y.-Z. Long, S. Ramakrishna, *J. Semicond.* **2019**, *40*, 111606.

[77] C. Yu, Q. Liu, Z. He, X. Gao, E. Wu, J. Guo, C. Zhou, Z. Feng, *J. Semicond.* **2020**, *41*, 032101.

[78] L. Li, C. Zhu, H. Liu, Y. Li, Q. Wang, K. Su, *Sensors* **2022**, *22*, 7751.

[79] P. Song, Z. Ma, J. Ma, L. Yang, J. Wei, Y. Zhao, M. Zhang, F. Yang, X. Wang, *Micromachines* **2016**, *11*, 56.

[80] C. Pang, G.-Y. Lee, T. Kim, S. M. Kim, H. N. Kim, S.-H. Ahn, K.-Y. Suh, *Nat. Mater.* **2012**, *11*, 795.

[81] M. Qu, D. Yang, X. Chen, D. Li, K. Zhu, J. Xie, in *2021 IEEE 34th Int. Conf. Micro Electro Mechanical Systems (MEMS)*, IEEE, Piscataway, NJ **2021**, pp. 59–63.

[82] S. Cai, W. Li, P. Xu, X. Xia, H. Yu, S. Zhang, X. Li, *Analyst* **2019**, *144*, 3729.

[83] S. Balasubramanian, S. R. Polaki, K. Prabakar, *Smart Mater. Struct.* **2020**, *29*, 095006.

[84] H. Debéda, I. Dufour, *Advanced Nanomaterials for Inexpensive Gas Microsensors: Synthesis, Integration and Applications*, Elsevier, Amsterdam **2020**, pp. 161–188.

[85] A. Zope, S.-S. Li, *Front. Mech. Eng.* **2022**, *8*, 898668.

[86] A. A. Zope, J.-H. Chang, T.-Y. Liu, S.-S. Li, *IEEE Trans. Electron Devices* **2020**, *67*, 1183.

[87] F. Hakim, N. G. Rudawski, T. Tharpe, R. Tabrizian, *Nat. Electron.* **2024**, *7*, 147.

[88] V. Pachkawade, Z. Tse, *Eng. Res. Express* **2022**, *4*, 022002.

[89] S. Bi, Q. Li, Z. He, Q. Guo, K. Asare-Yeboah, Y. Liu, C. Jiang, *Nano Energy* **2019**, *66*, 104101.

[90] F. Qiu, Y. Bai, D. Qu, G. Shan, L. Han, Y. Zhang, *Laser Phys.* **2023**, *33*, 115102.

[91] J. Shen, Y. Fan, Z. Xu, L. Wu, Y. Wang, X. Li, X. Gan, Y. Zhang, Y. Su, J. Shen, Z. Xu, Y. Zhang, Y. Su, Y. Fan, X. Li, L. Wu, Y. Wang, X. Gan, *Laser Photonics Rev.* **2022**, *17*, 2200248.

[92] C. Meng, P. C. V. Thrane, F. Ding, J. Gjessing, M. Thomaschewski, C. Wu, C. Dirdal, S. I. Bozhevolnyi, *Sci. Adv.* **2021**, *7*, eabg5639.

[93] C. A. Dirdal, P. C. V. Thrane, F. T. Dullo, J. Gjessing, A. Summanwar, J. Tschudi, *Opt. Lett.* **2022**, *47*, 1049.

[94] Y. Yang, Y. Liu, Y. Su, Y. Wang, Y. Zhang, H. Chen, L. Wang, Z. Wu, *Micromachines* **2024**, *15*, 235.

[95] C. Stoeckel, K. Meinel, M. Melzer, S. Zimmermann, R. Forke, K. Hiller, H. Kuhn, *Micromachines* **2022**, *13*, 625.

[96] M. Ramesh, M. Muthukrishnan, *Advanced Functional Piezoelectric Materials and Applications*, Vol. *131*, Materials Research Foundations, Millersville, PA **2022**, pp. 138–164.

[97] W. Jiang, F. M. Mayor, R. N. Patel, T. P. McKenna, C. J. Sarabalis, A. H. Safavi-Naeini, *Commun. Phys.* **2020**, *3*, 156.

[98] M. S. Rabbani, J. Churm, A. P. Feresidis, *IEEE Trans. Antennas Propag.* **2022**, *70*, 2439.

[99] P. H. Z. Cano, E. Vassos, Z. D. Zaharis, P. I. Lazaridis, T. V. Yioultsis, N. V. Kantartzis, A. P. Feresidis, *IEEE Trans. Antennas Propag.* **2024**, *72*, 1407.

[100] J. Wan, W. Yuan, Y. Chen, X. Zhu, M. Guo, P. Xu, *J. Mod. Opt.* **2021**, *68*, 1251.

[101] Q. Guo, R. Sekine, L. Ledezma, R. Nehra, D. J. Dean, A. Roy, R. M. Gray, S. Jahani, A. Marandi, *Nat. Photonics* **2022**, *16*, 625.

[102] Y. Liu, J. L. Benjamin, C. W. F. Parsonson, G. Zervas, *J. Lightwave Technol.* **2023**, *41*, 4882.

[103] W. Jiang, C. J. Sarabalis, Y. D. Dahmani, R. N. Patel, F. M. Mayor, T. P. McKenna, R. Van Laer, A. H. Safavi-Naeini, *Nat. Commun.* **2020**, *11*, 1166.

[104] Y. Ding, H. Wang, Y. Ji, *Opt. Laser Technol.* **2024**, *169*, 110028.

[105] X. Han, W. Fu, C. Zhong, C.-L. Zou, Y. Xu, A. Al Sayem, M. Xu, S. Wang, R. Cheng, L. Jiang, H. X. Tang, *Nat. Commun.* **2020**, *11*, 3237.

[106] V.-K. Wong, S. Mohamed Rabeek, S. Cheng Lai, M. Philibert, D. Boon Kiang Lim, S. Chen, M. Kumarasamy Raja, K. Yao, *Sensors* **2022**, *22*, 5724.

[107] C. Huang, D. Li, T. He, Y. Peng, W. Zhou, Z. Yang, J. Xu, Q. Wang, *ACS Photonics* **2020**, *7*, 3166.

[108] M. Kohli, D. Chelladurai, A. Messner, Y. Horst, D. Moor, J. Winiger, T. Blatter, T. Buriakova, C. Convertino, F. Eltes, M. Zervas, Y. Fedoryshyn, U. Koch, J. Leuthold, *J. Lightwave Technol.* **2023**, *41*, 3825.

[109] S. Vatani, B. Barahimi, M. Kazem Moravvej-Farshi, *Sci. Rep.* **2022**, *12*, 21490.

[110] T. Ma, G. Liu, L. Su, S. Liu, H. Liu, *Opt. Commun.* **2024**, *554*, 130221.

[111] A. Bekkali, H. Fujita, M. Hattori, *J. Lightwave Technol.* **2022**, *40*, 1509.

[112] H. Zheng, S. Lu, Q. Zhai, B. Huang, Y. Long, Y. Zhao, J. Qi, *J. Eng.* **2020**, *2020*, 141.

[113] Q. Lu, X. Chen, *Sci. Prog.* **2020**, *103*.

[114] C. Sun, Y. Liu, B. Li, W. Su, M. Luo, G. Du, Y. Wu, *Sensors* **2021**, *21*, 5513.

[115] A. Mekawy, M. Khalifa, T. A. Ali, A. H. Badawi, *IET Optoelectron.* **2019**, *13*, 134.

[116] X. Wang, X. Su, G. Liu, J. Han, R. Wang, K. Wang, *Opt. Express* **2021**, *29*, 41582.

[117] M. Kiuchi, N. Okimoto, Y. Hirata, G. Matsuoka, O. Torayashiki, in *2019 20th Int. Conf. Solid-State Sensors, Actuators and Microsystems & Eurosensors XXXIII (TRANSDUCERS & EUROSENSORS XXXIII)*, Berlin **2019**, pp. 1556–1559.

[118] P. Deng, T. Kane, X. Yuan, M. Wang, W. Xia, in *Tenth Int. Conf. Advances in Satellite and Space Communications. SPACOMM.* Athens **2018**.

[119] L. Yang, K. Yao, J. Wang, J. Cao, X. Lin, X. Liu, W. Liu, H. Gu, *Sci. Rep.* **2019**, *9*, 13150.

[120] Z. Hu, D. Jiang, X. Liu, B. Zhu, Q. Zeng, K. Qin, *Opt. Commun.* **2021**, *487*, 126802.

[121] A. Guignabert, T. Maillard, F. Barillot, O. Sosnicki, F. Claeyssen, in *AMS Conf.(US)*. Houston, TX **2021**.

[122] G. Gerlach, J. Mehner, T. Ozaki, N. Ohta, M. Fujiyoshi, *Sensors* **2022**, *22*, 4215.

[123] L. Qiao, X. Gao, K. Ren, C. Qiu, J. Liu, H. Jin, S. Dong, Z. Xu, F. Li, *Nat. Commun.* **2024**, *15*, 805.

[124] V. Mai, H. Kim, *Opt. Commun.* **2023**, *527*, 128963.

[125] H. Gowda, B. Gowda, U. Wallrabe, *Micromachines* **2019**, *10*, 797.

[126] S. A. Moosavi, M. Quintavalla, J. Mocci, R. Muradore, H. Saghafifar, S. Bonora, *Opt. Lett.* **2019**, *44*, 606.

[127] Z. Yang, J. Lu, M. ZhuGe, Y. Cheng, J. Hu, F. Li, S. Qiao, Y. Zhang, G. Hu, Q. Yang, D. Peng, K. Liu, C. Pan, *Adv. Mater.* **2019**, *31*, 1900647.

[128] J. Lu, C. Xu, F. Li, Z. Yang, Y. Peng, X. Li, M. Que, C. Pan, Z. L. Wang, *ACS Nano* **2018**, *12*, 11899.

[129] J. Lu, Z. Yang, F. Li, M. Jiang, Y. Zhang, J. Sun, G. Hu, Q. Xu, C. Xu, C. Pan, Z. L. Wang, *Mater. Today* **2019**, *24*, 33.

[130] K. D. Zeuner, M. Paul, T. Lettner, C. Reuterskiöld Hedlund, L. Schweickert, S. Steinhauer, L. Yang, J. Zichi, M. Hammar, K. D. Jöns, V. Zwiller, *Appl. Phys. Lett.* **2018**, *112*, 173102.

[131] M. Moczała-Dusanowska, Ł. Dusanowski, O. Iff, T. Huber, S. Kuhn, T. Czyszanowski, C. Schneider, S. Höfling, *ACS Photonics* **2020**, *7*, 3474.

[132] J. Liu, R. Su, Y. Wei, B. Yao, S. F. C. da Silva, Y. Yu, J. Iles-Smith, K. Srinivasan, A. Rastelli, J. Li, X. Wang, *Nat. Nanotechnol.* **2019**, *14*, 586.

[133] N. G. Chatzarakis, S. Germanis, I. Thyris, C. Katsidis, A. Stavrinidis, G. Konstantinidis, Z. Hatzopoulos, N. T. Pelekanos, *Phys. Rev. Appl.* **2023**, *20*, 34011.

[134] N. Tomm, A. Javadi, N. O. Antoniadis, D. Najer, M. C. Löbl, A. R. Korsch, R. Schott, S. R. Valentin, A. D. Wieck, A. Ludwig, R. J. Warburton, *Nat. Nanotechnol.* **2021**, *16*, 399.

[135] R. Uppu, H. T. Eriksen, H. Thyrrestrup, A. D. Uğurlu, Y. Wang, S. Scholz, A. D. Wieck, A. Ludwig, M. C. Löbl, R. J. Warburton, P. Lodahl, L. Midolo, *Nat. Commun.* **2020**, *11*, 3782.

[136] R. Ghaffarivardavagh, S. Saad Afzal, O. Rodriguez, F. Adib, in *Proc. Annual Conf. ACM Special Interest Group on Data Communication on the Applications, Technologies, Architectures, and Protocols for Computer Communication*, Vol. *722*, ACM, New York **2020**, p. 722.

[137] Z. Tian, L. Su, H. Wang, H. Wang, Y. Zi, *Adv. Opt. Mater.* **2022**, *10*, 2102091.

[138] S. F. Nabavi, A. Farshidianfar, A. Afsharfard, H. H. Khodaparast, *Int. J. Mech. Sci.* **2019**, *151*, 498.

[139] P. Han, G. Pan, B. Zhang, W. Wang, W. Tian, *Ocean Eng.* **2020**, *211*, 107619.

[140] W. S. Hwang, J. H. Ahn, S. Y. Jeong, H. J. Jung, S. K. Hong, J. Y. Choi, J. Y. Cho, J. H. Kim, T. H. Sung, *Sens. Actuators, A* **2017**, *260*, 191.

[141] A. Pregowska, M. Perkins, Artificial Intelligence in Medical Education: Technology and Ethical Risk, https://ssrn.com/abstract=4643763 (accessed: December 2023).

[142] Z. Rudnicka, J. Szczepanski, A. Pregowska, *Electronics* **2024**, *13*, 746.

[143] Z. Rudnicka, K. Proniewska, M. Perkins, A. Pregowska, *Electronics* **2024**, *13*, 866.

[144] K. Guo, Z. Yang, C.-H. Yu, M. J. Buehler, *Mater. Horiz.* **2021**, *8*, 1153.

[145] D. Wang, M. Zhang, *Front. Commun. Networks* **2021**, *2*, 656786.

[146] R. Thapa, S. Poudel, K. Krukiewicz, A. Kunwar, *Measurement* **2024**, *227*, 114123.

[147] Q. Shi, Z. Zhang, T. Chen, C. Lee, *Nano Energy* **2019**, *62*, 355.

[148] Z. Yang, Z. Zhu, Z. Chen, M. Liu, B. Zhao, Y. Liu, Z. Cheng, S. Wang, W. Yang, T. Yu, C. K. Jeong, *Sensors* **2021**, *21*, 8422.

[149] Q. Zhou, Y. Shi, Z. Xu, R. Qu, G. Xu, *IEEE Access* **2020**, *8*, 101309.

[150] M. Zhu, Z. Sun, Z. Zhang, Q. Shi, T. He, H. Liu, T. Chen, C. Lee, *Sci. Adv.* **2020**, *6*, eaaz8693.

[151] Y. Kim, P. Panda, *Sci. Rep.* **2021**, *11*, 19037.

[152] D. Kim, Z. Yang, J. Cho, D. Park, H. K. Dong, J. Lee, S. Ryu, S.-W. Kim, M. Kim, *EcoMat* **2023**, *5*, e12384.

[153] H. Askari, N. Xu, B. H. Groenner Barbosa, Y. Huang, L. Chen, A. Khajepour, H. Chen, Z. L. Wang, *Mater. Today* **2022**, *52*, 188.

[154] P. Tan, Y. Xi, S. Chao, D. Jiang, Z. Liu, Y. Fan, Z. Li, *Biosensors* **2022**, *12*, 234.

[155] K. Meng, J. Chen, X. Li, Y. Wu, W. Fan, Z. Zhou, Q. He, X. Wang, X. Fan, Y. Zhang, J. Yang, Z. L. Wang, *Wearable Electron.* **2019**, *29*, 1806388.

[156] X. Ji, T. Zhao, X. Zhao, X. Lu, T. Li, *Adv. Mater. Technol.* **2020**, *5*, 1900921.

[157] X. Zhao, Z. Zhang, L. Xu, F. Gao, B. Zhao, T. Ouyang, Z. Kang, Q. Liao, Y. Zhang, *Nano Energy* **2021**, *85*, 106001.

[158] L. S. Fang, C. Y. Tsai, M. H. Xu, S. W. Wu, W. C. Lo, Y. H. Lu, Y. K. Fuh, *Nanotechnology* **2020**, *31*, 155502.

[159] W. Xie, H. Chen, J. Wei, J. Zhang, Q. Zhang, *Proc. ACM Interact. Mobile Wearable Ubiquitous Technol.* **2024**, *7*, 1.

[160] S. Li, W. Peng, J. Wang, L. Lin, Y. Zi, G. Zhang, Z. L. Wang, *ACS Nano* **2016**, *10*, 7973.

[161] A. Ahmed, S. L. Zhang, I. Hassan, Z. Saadatnia, Y. Zi, J. Zu, Z. L. Wang, *Extreme Mech. Lett.* **2017**, *13*, 25.

[162] G. Zhao, J. Yang, J. Chen, G. Zhu, Z. Jiang, X. Liu, G. Niu, Z. L. Wang, B. Zhang, *Adv. Mater. Technol.* **2019**, *4*, 1800167.

[163] T. Guo, J. Zhao, W. Liu, G. Liu, Y. Pang, T. Bu, F. Xi, C. Zhang, X. Li, X. Li, J. Zhao, W. Liu, G. Liu, Y. Pang, T. Bu, F. Xi, C. Zhang, *Adv. Mater. Technol.* **2018**, *3*, 1800140.

[164] C. Sukumaran, V. Vivekananthan, V. Mohan, Z. C. Alex, A. Chandrasekhar, S. J. Kim, *Appl. Mater. Today* **2020**, *19*, 100625.

[165] M. He, Z. Liang, Y. Wang, J. Yan, X. Qing, F. Wang, *Measurement* **2024**, *225*, 114052.

[166] G. Cosoli, M. T. Calcagni, G. Salerno, A. Mancini, G. Narang, A. Galdelli, A. Mobili, F. Tittarelli, G. M. Revel, *Sensors* **2024**, *24*, 572.

[167] A. Ali, S. Ali, H. Shaukat, E. Khalid, L. Behram, H. Rani, W. A. Altabey, S. A. Kouritem, M. Noori, *Results Eng.* **2024**, *21*, 101777.

[168] Z. Zheng, X. Wang, G. Hang, J. Duan, J. Zhang, W. Zhang, Z. Liu, *Renewable Sustainable Energy Rev.* **2024**, *193*, 114285.

[169] P. Li, Y. Fan, Z. Liu, B. Tian, Z. Wang, D. Li, Z. Han, Z. Zhang, F. Xiong, *IET Sci. Meas. Technol.* **2024**, *18*, 145.

[170] D. Tang, Y. Zhou, X. Cui, Y. Zhang, *Cyber-Phys. Syst.* **2024**, *4*, 77.

[171] A. Zazzi, A. D. Das, L. Hüssen, R. Negra, J. Witzens, *Photonics Res.* **2024**, *12*, 85.

[172] Y. H. Jung, S. K. Hong, H. S. Wang, J. H. Han, T. X. Pham, H. Park, J. Kim, S. Kang, C. D. Yoo, K. J. Lee, *Adv. Mater.* **2019**, *32*, 1904020.

[173] M. M. Abolhasani, K. Shirvanimoghaddam, H. Khayyam, S. M. Moosavi, N. Zohdi, M. Naebe, *Polym. Test.* **2018**, *66*, 178.

[174] M. Shabara, A. Rahman Badawi, T.-B. Xu, in *AIAA Scitech 2020 Forum*, AIAA SciTech Forum, American Institute of Aeronautics and Astronautics, Reston, VA **2020**.

[175] S. Bagheri, N. Wu, S. Filizadeh, *Smart Mater. Struct.* **2020**, *29*, 105004.

[176] P. Jiao, *Nano Energy* **2021**, *88*, 106227.

[177] S. Nabavi, L. Zhang, *Proc. (MDPI)* **2018**, *2*, 930.

[178] P. V. Bhosale, S. D. Agashe, *Noise Vibr. Worldwide* **2023**, *55*, 3.

[179] M. Badás, P. Piron, J. Bouwmeester, J. Loicq, H. Kuiper, E. Gill, *Opt. Eng.* **2023**, *63*, 041206.

[180] Y. Wu, Y. Ma, H. Zheng, S. Ramakrishna, *Mater. Des.* **2021**, *211*, 110164.

[181] J. L. Edmunds, S. Sonmezoglu, M. M. Maharbiz, *Opt. Express* **2022**, *30*, 43664.

[182] Y. Tao, W. Y. Liu, C. Nan, S. X. Wang, X. S. Ding, L. Liu, Y. Bai, Y. R. Zhou, E. B. Xing, J. Chen, J. Tang, J. Liu, *Opt. Commun.* **2024**, *556*, 130264.

[183] M. Dutta, S. Betal, X. G. Peralta, A. S. Bhalla, R. Guo, *Sci. Rep.* **2016**, *6*, 38041.

[184] J. Lin, Y. Wang, R. Xiong, B. Sa, C. Shi, J. Zhai, Z. Fang, K. Zhu, F. Yan, H. Tian, G. Ge, G. Li, H. Bai, P. Wang, Y. Zhang, X. Wu, *Acta Mater.* **2022**, *235*, 118061.

[185] J. Yang, Z. Li, X. Xin, X. Gao, X. Yuan, Z. Wang, Z. Yu, X. Wang, J. Zhou, S. Dong, *Sci. Adv.* **2019**, *5*, eaax1782.

[186] H. Cui, R. Hensleigh, D. Yao, D. Maurya, P. Kumar, M. G. Kang, S. Priya, *Nat. Mater.* **2019**, *18*, 234.

[187] Z.-D. Zhang, S.-Y. Yu, H. Xu, M.-H. Lu, Y.-F. Chen, *Adv. Mater.* **2024**, *36*, 2312861.

[188] S. A. Giannuzzi, T. Myers, S. Pietrowski, J. L. Kauffman, in *AIAA SCITECH 2024 Forum, AIAA SciTech Forum*, American Institute of Aeronautics and Astronautics, Orlando, FL **2024**.

[189] P. M. Ferreira, M. A. Machado, C. Vidal, M. S. Carvalho, *Adv. Eng. Software* **2024**, *193*, 103651.

[190] S. M. Shree, V. C. Shamritha, I. Malar, in *2024 Ninth Int. Conf. Science Technology Engineering and Mathematics (ICONSTEM)* Chennai **2024**, pp. 1–7.

[191] J. Hao, N. Ahmad Nizam Nik Malek, W. Hairul Anuar Kamaruddin, J. Li, C. Jianhua Hao, *BMEMat* **2024**, *2*, e12087.

[192] A. Khan, R. Joshi, M. K. Sharma, C.-J. Huang, J.-H. Yu, Y.-L. Wang, Z.-H. Lin, *Nano Trends* **2024**, *6*, 100032.

[193] K. V. Amith, R. C. Kamath, *Eng. Proc.* **2023**, *59*, 21.

[194] Z. Shi, L. Meng, X. Shi, H. Li, J. Zhang, Q. Sun, X. Liu, J. Chen, S. Liu, *Nano-Micro Lett.* **2022**, *14*, 141.

[195] Y. Wu, H. Chen, N. Sun, Z. Fan, Y. Fang, *Int. J. Robust Nonlinear Control* **2023**, *33*, 2251.

[196] M. Huang, M. Zhu, X. Feng, Z. Zhang, T. Tang, X. Guo, T. Chen, H. Liu, L. Sun, C. Lee, *ACS Nano* **2023**, *17*, 6435.

[197] M. R. P. Elenchezhian, V. Vadlamudi, R. Raihan, K. Reifsnider, E. Reifsnider, *Smart Mater. Struct.* **2021**, *30*, 083001.

[198] X. Wu, X. Li, P. Qi, C. Zhang, J. Luo, *Smart Mater. Struct.* **2024**, *33*, 025026.

[199] Z. Gao, H. Ning, C. Chen, R. Wilson, B. Shi, H. Ye, H. Yan, M. J. Reece, *J. Am. Ceram. Soc.* **2013**, *96*, 1163.

[200] A. Yadegari, M. Akbarzadeh, F. Kargaran, R. Mirzaee, I. Salahshoori, M. A. L. Nobre, H. A. Khonakdar, *J. Mater. Chem. B* **2024**, *12*, 5272.

[201] Y. Meng, G. Chen, M. Huang, *Nanomaterials* **2022**, *12*, 1171.

[202] A. Kumar, W. Kim, P. Sriboriboon, H. Y. Lee, Y. Kim, J. Ryu, *Sens. Actuators, A* **2024**, *372*, 115342.

[203] P. Muralt, J. Conde, A. Artieda, F. Martin, M. Cantoni, *Int. J. Microwave Wireless Technol.* **2009**, *1*, 19.

[204] M. Zgonik, P. Bernasconi, M. Duelli, R. Schlesser, P. Günter, M. H. Garrett, D. Rytz, Y. Zhu, X. Wu, *Phys. Rev. B* **1994**, *50*, 5941.

[205] V. T. Tùng, N. T. Tinh, N. H. Yen, D. A. Tuan, *Int. J. Mater. Chem.* **2013**, *3*, 4.

[206] L. Khine, *Performance Parameters of Micromechanical Resonators*, National University of Singapore, Singapore **2010**.

[207] T. Li, P. S. Lee, *Small Struct.* **2022**, *3*, 2100128.

[208] S. Bairagi, M. Shahadat, D. M. Mulvihill, W. Ali, *Nano Energy* **2023**, *111*, 108414.

[209] Y. H. Jung, J. An, D. Y. Hyeon, H. S. Wang, I. Kim, C. K. Jeong, K.-I. Park, P. S. Lee, K. J. Lee, *Adv. Funct. Mater.* **2023**, *34*, 2309316.

[210] B. Hu, W. Liu, Y. Liu, C. Yang, Z. Wang, L. Lu, Y. Cai, S. Guo, C. Sun, *IEEE Trans. Electron Devices* **2024**, *71*, 3162.

[211] A. Rahaman, C. H. Park, B. Kim, *Sens. Actuators, A* **2020**, *311*, 112087.

[212] A. Di Gaspare, E. Arianna Aurelia Pogna, L. Salemi, O. Balci, A. Ronieri Cadore, S. Maruti Shinde, L. Li, C. di Franco, A. Giles Davies, E. Harold Linfield, A. Carlo Ferrari, G. Scamarcio, M. Serena Vitiello, *Adv. Funct. Mater.* **2020**, *31*, 2008039.

[213] L. Chen, H. Liu, H. Qi, J. Chen, *Prog. Mater. Sci.* **2022**, *127*, 100944.

[214] L. Thylén, U. Westergren, P. Holmström, R. Schatz, P. Jänes, 7 - Recent developments in high-speed optical modulators. Ivan P. Kaminow, Tingye Li, Alan E. Willner *Optical Fiber Telecommunications VA: Components and Subsystems* Academic Press **2008**, pp. 183–220.

[215] M. Cheng, G. Zhu, F. Zhang, W. Lai Tang, S. Jianping, J. Quan Yang, L. Ya Zhu, *J. Adv. Res.* **2020**, *26*, 53.

[216] A. Arbie, Z. A. Hasan, A. W. Nuayi, *J. Energy* **2021**, *2021*, 7258449.

[217] D. Huang, P. Pintus, C. Zhang, Y. Shoji, T. Mizumoto, J. E. Bowers, *IEEE J. Sel. Top. Quantum Electron.* **2016**, *22*, 271.

[218] O. Atalar, R. Van Laer, A. H. Safavi-Naeini, A. Arbabian, *Nat. Commun.* **2022**, *13*, 1526.

[219] Z. Chen, L. Song, W. Cao, *J. Mater. Res. Technol.* **2023**, *23*, 5040.

[220] Z. Chew, L. Li, *Sens. Actuators, A* **2010**, *162*, 82.

[221] F. Akasheh, J. D. Fraser, S. Bose, A. Bandyopadhyay, *IEEE Trans. Ultrason. Ferroelectr. Freq. Control* **2005**, *52*, 455.

[222] M. Skalský, Z. Havránek, J. Fialka, *Sensors* **2019**, *19*, 1710.

[223] M. S. Salem, S. Ahmed, A. Shaker, M. T. Alshammari, K. A. Al-Dhlan, A. Alanazi, A. Saeed, M. Abouelatta, *Micromachines* **2021**, *12*, 973.

[224] D. M. B. Lesko, A. J. Lind, N. Hoghooghi, A. Kowligy, H. Timmers, P. Sekhar, B. Rudin, F. Emaury, G. B. Rieker, S. A. Diddams, *OSA Continuum* **2020**, *3*, 2070.

[225] G. Sharma, S. Kumar, D. Kumar, V. Singh, *Opt. Appl.* **2015**, *45*, 491.

[226] N. Hosseini, R. Dekker, M. Hoekman, M. Dekkers, J. Bos, A. Leinse, R. Heideman, *Opt. Express* **2015**, *23*, 14018.

[227] M. Tian, L. Xu, Y. Yang, M. Tian, Y. Yang, L. Xu, *Adv. Electron. Mater.* **2022**, *8*, 2101409.

[228] A. Kausar, C.-Y. Chang, M. Asif, Z. Raja, A. Zameer, M. Shoaib, *Eur. Phys. J. Plus* **2024**, *139*, 16.

[229] Z. Sun, M. Zhu, Z. Zhang, Z. Chen, Q. Shi, X. Shan, R. Chen, H. Yeow, C. Lee, *Adv. Sci.* **2021**, *8*, 2100230.

[230] F. Wen, Z. Zhang, T. He, C. Lee, *Nat. Commun.* **2021**, *12*, 5378.

[231] A. Ruiz, J. L. Emeterio, A. Ramos, *Integr. Ferroelectr.* **2004**, *63*, 137.

[232] Z. Zhou, K. Chen, X. Li, S. Zhang, Y. Wu, Y. Zhou, K. Meng, C. Sun, Q. He, W. Fan, E. Fan, Z. Lin, X. Tan, W. Deng, J. Yang, J. Chen, *Nat. Electron.* **2020**, *3*, 571.

[233] T. Li, Y. Su, H. Zheng, F. Chen, X. Li, Y. Tan, Z. Zhou, *Adv. Intell. Syst.* **2023**, *5*, 2200460.

[234] X. Fang, P. Yan, *IEEE Trans. Med. Imaging* **2020**, *39*, 3619.

Agata Roszkiewicz, Ph.D., Eng., graduated from the Faculty of Technical Physics at the Warsaw University of Technology in 2006. She earned her Ph.D. with distinction from the Institute of Fundamental Technological Research (IFTR PAS) in 2012 for her work on surface plasmon polaritons at periodic structures. Since then, she has been a researcher at IFTR PAS. Her research focuses on numerical and theoretical aspects of plasmonics and nanophotonics, as well as experimental surface research using AFM. In 2014, she received the award of the Academies of the Visegrad Group countries for a young scientist in the field of applied mathematics.

Magdalena Garlińska, Ph.D., MBA., while working at the Military University of Technology, her research focused on developing wireless optical communication systems. In 2015, she participated in the Top500 Innovators program at the University of Cambridge and the University of Oxford. She is also a graduate of the MBA program at the Polish-Japanese Academy of Information Technology. Additionally, she holds a postgraduate degree in innovation management from the Warsaw School of Economics. She is an expert in assessing funding applications for R&D projects under European and national programs. Since March 2023, she has been working at the Łukasiewicz Center in the Commercialization Department.

Agnieszka Pregowska received her Ph.D., D.Sc., and Eng. from the Institute of Fundamental Technological Research Polish Academy of Sciences. She is a graduate of the Faculty of Mechatronics at the Warsaw University of Technology (2008). She obtained a Ph.D. degree for research in controlling and optimizing the dynamics of systems, at the Polish Academy of Sciences, IPPT PAN (2013). She achieved habilitation in informatics for results in neuroinformatics in 2023. Her scientific interests focus on developing the concepts of information theory and biologically inspired artificial intelligence and their applications in the processing and classification of biomedical data as well as neural network security. She is also involved in the development of extended reality in medicine and medical education.